Biochimica et Biophysica Acta 1853 (2015) 1416–1428

Contents lists available at ScienceDirect

Biochimica et Biophysica Acta

journal homepage: www.elsevier.com/locate/bbamcr

Review

Tangled web of interactions among proteins involved in iron–sulfur cluster assembly as unraveled by NMR, SAXS, chemical crosslinking, and functional studies ☆

Jin Hae Kim [1], Jameson R. Bothe, T. Reid Alderson [2], John L. Markley *

Biochemistry Department, University of Wisconsin-Madison, Madison, WI 53706, USA

ARTICLE INFO

Article history:
Received 3 July 2014
Received in revised form 18 October 2014
Accepted 13 November 2014
Available online 22 November 2014

Keywords:
Iron–sulfur cluster biosynthesis
Conformational equilibria
Protein–protein interactions
Nuclear magnetic resonance (NMR) spectroscopy
Small-angle X-ray scattering (SAXS)

ABSTRACT

Proteins containing iron–sulfur (Fe–S) clusters arose early in evolution and are essential to life. Organisms have evolved machinery consisting of specialized proteins that operate together to assemble Fe–S clusters efficiently so as to minimize cellular exposure to their toxic constituents: iron and sulfide ions. To date, the best studied system is the iron-sulfur cluster (*isc*) operon of *Escherichia coli*, and the eight ISC proteins it encodes. Our investigations over the past five years have identified two functional conformational states for the scaffold protein (IscU) and have shown that the other ISC proteins that interact with IscU prefer to bind one conformational state or the other. From analyses of the NMR spectroscopy-derived network of interactions of ISC proteins, small-angle X-ray scattering (SAXS) data, chemical crosslinking experiments, and functional assays, we have constructed working models for Fe–S cluster assembly and delivery. Future work is needed to validate and refine what has been learned about the *E. coli* system and to extend these findings to the homologous Fe–S cluster biosynthetic machinery of yeast and human mitochondria. This article is part of a Special Issue entitled: Fe/S proteins: Analysis, structure, function, biogenesis and diseases.

1. Introduction

1.1. Ancient earth: an iron–sulfur world

Owing to the natural abundance and unique chemical and electronic properties of iron (Fe) and sulfur (S) [1], it has been hypothesized that ancient organisms arose from an anaerobic, Fe–S world [2,3]. Recent organic syntheses conducted at high temperatures and pressures in the presence of H_2S and Fe catalysts have successfully converted carbon monoxide into peptides [4,5], and thereby created essential C–C bonds and metabolites (e.g. pyruvate) [6] required for energy acquisition and the biosynthesis of amino acids and nucleotides — the sustenance of life. Evolutionary evidence in support of the Fe–S world theory manifests in certain metabolic pathways (e.g. glucose oxidation) of primitive archaebacteria and thermophiles, which rely on Fe–S clusters, whereas contemporary eubacteria have evolved to utilize NAD(P)H and NAD(P) and phosphorylation cascades [7]. Yet, while modern organisms have since developed other, non-Fe–S-based mechanisms for redox-based metabolism, Fe–S clusters comprise a common class of enzymatic cofactors that represent evolutionary relics from the ancient Fe–S world.

1.2. Fe–S clusters in modern biochemistry

Fe–S clusters constitute a ubiquitous class of protein prosthetic groups essential to life [8]. Following the discovery of ferredoxins as Fe–S cluster containing proteins in the 1960s [9], the diverse chemical, electronic, and magnetic properties of Fe–S clusters were thoroughly characterized in vitro, and numerous synthetic routes for preparing Fe–S clusters of various chemical compositions have been documented [8]. The most common Fe–S cluster types are [2Fe–2S], [3Fe–4S], and [4Fe–4S] ligated to proteins through cysteine, histidine, or aspartate residues. Fe–S clusters confer unique functional properties to proteins involved in vital cellular processes, including metabolism [10], photosynthesis [11], DNA replication and repair [12–15], and nitrogen fixation [16].

Fe–S clusters form spontaneously under anaerobic conditions in vitro; however, under oxidizing conditions in vivo, oxygen-labile Fe–S clusters require intricate proteinaceous machinery for their efficient synthesis and transfer to apoproteins [10,17,18]. Molecular oxygen rapidly degrades Fe–S clusters, and the resultant free iron ions, via Fenton chemistry, produce reactive oxygen species (ROS; e.g. hydroxyl

☆ This article is part of a Special Issue entitled: Fe/S proteins: Analysis, structure, function, biogenesis and diseases.

* Corresponding author at: Biochemistry Department, University of Wisconsin-Madison, 433 Babcock Drive, Madison, WI 53706, USA.
E-mail address: jmarkley@wisc.edu (J.L. Markley).
[1] Current addresses: Max Planck Institute for Biophysical Chemistry, Göttingen, Germany.
[2] Current addresses: Laboratory of Chemical Physics, National Institutes of Health, Bethesda, MD, USA, and Department of Chemistry, University of Oxford, Oxford, UK.

http://dx.doi.org/10.1016/j.bbamcr.2014.11.020

radicals) that can inflict irreversible macromolecular damage [19], ultimately culminating in cell death.

Prokaryotes possess three distinct biosynthetic systems to securely assemble and deliver Fe–S clusters: the nitrogen-fixation system (NIF), the sulfur-mobilization machinery (SUF), and the ISC-assembly system. The ISC-assembly machinery produces the majority of Fe–S clusters needed for cellular activity, whereas the NIF and SUF systems play specialized roles in the maturation of nitrogenase and the oxidative stress response, respectively [20].

1.3. Fe–S cluster biosynthesis and human health

Eukaryotes contain homologous ISC-assembly proteins within their mitochondria, and these dedicated proteins, along with the cytosolic Fe–S cluster assembly (CIA) system, produce nearly all nuclear, cytosolic, mitochondrial, and endoplasmic reticulum-based Fe–S proteins [21,22]. Of utmost importance to the maintenance of organismal health, apoprotein targets that require Fe–S cluster delivery include DNA helicases, DNA polymerases, transcription factors, mismatch repair proteins, and complexes I–III of the electron transport chain [21]. Defects in eukaryotic ISC-assembly machinery thus manifest as a variety of diseases, including myopathies (e.g. mitochondrial encephalomyopathy) and neurodegenerative diseases (e.g. Friedreich's ataxia) [23–25]. Recent evidence also suggests that defective ISC biogenesis may play a role in the onset and progression of Parkinson's disease [26,27], owing to the propensity with which degraded ISCs form ROS that lead to oxidative damage in the brains of Parkinson's disease patients.

1.4. Model systems for Fe–S cluster biosynthesis and transfer

Proteins associated with Fe–S cluster biogenesis and Fe–S protein maturation play vital physiological roles, and the mechanisms of their biosynthesis have been investigated intensively. Studies in bacteria (*Azotobacter vinelandii*) [28–30] and yeast (*Saccharomyces cerevisiae*) [31–33] have greatly advanced our understanding of Fe–S protein maturation. However, *Escherichia coli* has emerged as the model organism providing the greatest insight into the mechanistic details for Fe–S cluster biosynthesis and delivery to apoproteins [34,35]. The proteins encoded by the *isc* operon of *E. coli* (Fig. 1) [30,36] comprise IscR (transcription factor that regulates the expression of the *iscRSUA* operon in response to the iron–sulfur cluster content of the cell [37]), IscS (PLP-dependent cysteine desulfurase), IscU (scaffold for ISC assembly), IscA (alternate scaffold/possible iron-delivery protein), HscB (Hsp40 J-type co-chaperone), HscA (specialized Hsp70 chaperone), Fdx ([2Fe–2S] ferredoxin), and IscX (iron binding protein and possible iron donor in Fe–S cluster biosynthesis). Intensive biochemical [38] and structural [39] studies have elucidated many of the steps involved in Fe–S cluster biosynthesis on IscU and have shown that the process is inhibited by the bacterial frataxin protein (CyaY), whose gene is external to the *isc* operon [40,41].

1.5. High-resolution, structural analyses of the ISC proteins

Three-dimensional structures of ISC proteins and their complexes (Table 1) have provided important insight into the process of Fe–S cluster biosynthesis and transfer.

1.6. IscU

IscU is a scaffold protein on which Fe–S clusters are assembled and sustained until transferred to target proteins. IscU contains three highly-conserved and physiologically essential cysteine residues, a conserved histidine residue, and a conserved 'LPPVK' motif [10]. Conflicting evidence has been reported regarding the types of Fe–S clusters assembled on IscU. In vitro studies of *A. vinelandii* IscU showed that [2Fe–2S] clusters are assembled first by IscS-mediated reconstitution, and that reductive coupling between two [2Fe–2S] clusters produces one [4Fe–4S] cluster [42], which can be transferred subsequently to apo-aconitase [43].

1.7. IscA

The physiological function of IscA has yet to be definitively determined. IscA has been proposed to function as a scaffold for assembling Fe–S clusters, but IscA also has a high affinity for iron ions. Thus, IscA may be an alternative scaffold protein for Fe–S cluster assembly and transfer [44,45], or it may serve as an iron-delivery protein [46,47]. In eukaryotes, however, genetic and biochemical studies have indicated that Isa1 and Isa2, the yeast isoforms of bacterial IscA, play important roles in producing mature mitochondrial aconitase-like proteins (Aco1 and Lys4) [48], the mitochondrial SAM-dependent biotin synthase (Bio2) [49], and lipoic acid synthase (Lip5); these results support the hypothesis that IscA acts as an Fe–S cluster scaffold protein [18].

1.8. HscB

HscB is an Hsp40-type co-chaperone protein consisting of two domains. The C-terminal domain is involved in binding the substrate, IscU, whereas the N-terminal J-domain is responsible for interacting with HscA and stimulating its ATPase activity during Fe–S cluster transfer [50].

1.9. HscA

HscA is the Hsp70-type chaperone protein with ATPase activity that binds to IscU in the canonical Hsp70 nucleotide-dependent manner.

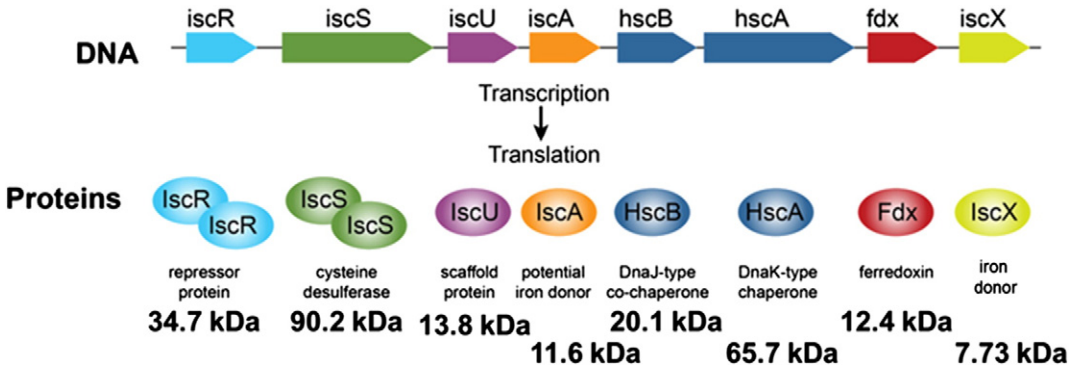

Fig. 1. The *isc* operon and the ISC proteins it encodes.

Table 1
Proteins involved in iron–sulfur cluster assembly and relevant structural information.

Protein	Comment	Organism	PDB code (method)	Reference
IscU	Scaffold protein	*E. coli*	2l4x (NMR)	[101]
IscU(D39A)	Scaffold protein variant with stabilized S-state	*E. coli*	2kqk (NMR)	[101]
IscU(D39A):[2Fe–2S]	Holo scaffold protein (substitution homologous to D39A in *E. coli*)	*Aquifex aeolicus*	2z7e (X-ray)	[78]
IscU:Zn complex	Inhibited form of IscU	*Haemophilus influenzae*	1rp9 (NMR)	[77]
IscU:Zn complex	Inhibited form of IscU	*Thermus thermophilus*	2qq4 (X-ray)	[76]
IscU:Zn complex	Inhibited form of IscU	*Streptococcus pyogenes*	1su0 (X-ray)	[75]
IscS	Cysteine desulfurase: $(IscS)_2$ homodimer	*E. coli*	1p3w (X-ray)	[136]
IscU–IscS complex	$(IscU)_2$–$(IscS)_2$	*E. coli*	3lvl (X-ray)	[61]
IscU(D39A):[2Fe–2S] complex	$(IscU:[2Fe–2S])_2$–$(IscS)_2$	*Archaeoglobus fulgidus*	4eb5 (X-ray)	[68]
IscU(D39A):[2Fe–2S] complex	Oxidatively degraded	*Archaeoglobus fulgidus*	4eb7 (X-ray)	[68]
IscA(1–105)	Iron delivery, alternative scaffold; homo-tetramer, Hg derivative	*E. coli*	1r94 (X-ray)	[137]
IscA(1–107)	Iron delivery, alternative scaffold; homo-tetramer, apo-protein	*E. coli*	1s98 (X-ray)	[138]
IscA(1–116)	Iron delivery, alternative scaffold; monomer	*Aquifex aeolicus*	1nwb (NMR)	[139]
IscX (aka YfhJ)	Iron delivery, or frataxin-like regulator of cluster assembly?	*E. coli*	1uj8 (X-ray)	[140]
IscX	Iron delivery, or frataxin-like regulator of cluster assembly?	*E. coli*	2bzt (NMR)	[56]
CyaY bacterial frataxin	Inhibitor of cluster assembly	*E. coli*	1ew4 (X-ray)	[141]
CyaY bacterial frataxin–iron complex	Iron delivery protein?	*E. coli*	1soy (NMR)	[142]
YFH1 yeast frataxin	Iron delivery protein	*Saccharomyces cerevisiae*	1xaq (NMR)	[143]
YFH1 yeast frataxin (trimeric)	Iron delivery protein	*Saccharomyces cerevisiae*	2fql (X-ray)	[144]
YFH1 yeast frataxin (trimeric)	Iron delivery protein	*Saccharomyces cerevisiae*	3oeq (X-ray)	[145]
YFH1 yeast frataxin (trimeric, cobalt complex)	Iron delivery protein	*Saccharomyces cerevisiae*	3oer (X-ray)	[145]
YFH1 yeast frataxin (trimeric, Fe^{2+} complex)	Iron delivery protein	*Saccharomyces cerevisiae*	4ec2 (X-ray)	[146]
FRDA (frataxin)	Enhances desulfurase activity	*Homo sapiens*	1ekg (X-ray)	[147]
FRDA (frataxin)	Enhances desulfurase activity	*Homo sapiens*	1ly7 (NMR)	[148]
HscA(390–615)–peptide complex	Chaperone (DnaK-type protein) substrate binding domain with bound IscU peptide	*E. coli*	1u00 (X-ray)	[93]
HscB	Co-chaperone (DnaJ-type protein)	*E. coli*	1fpo (X-ray)	[149]
HSC20	Co-chaperone (DnaJ-type protein)	*Homo sapiens*	3bvo (X-ray)	[150]
Fdx (ferredoxin)	Electron transfer	*E. coli*	1i7h (X-ray)	[151]
IscR	Apo-repressor protein; homodimer	*E. coli*	4hf0 (X-ray)	[152]
IscR–DNA complex	Homodimer with bound HYA promoter fragment	*E. coli*	4chu (X-ray)	[153]

Along with HscB, HscA facilitates Fe–S cluster transfer from holo-IscU to an acceptor apoprotein [51].

1.10. Ferredoxin (Fdx)

Fdx contains a [2Fe–2S] cluster coordinated by four conserved cysteine residues. Studies of yeast [2Fe–2S] Fdx (Yah1) have suggested that this protein may deliver electrons required for Fe–S cluster assembly [52,53]. Studies of in vitro cluster assembly have shown that the Fe–S cluster assembled on IscU can be transferred to the apo-form of Fdx [45,54,55], implying that [2Fe–2S] Fdx is one of the target proteins to which the ISC system supplies an Fe–S cluster.

1.11. IscX

IscX (also known as YfhJ) is a small acidic protein whose physiological role has been unclear [36]. It has been shown to form a complex with IscS and also to have iron-binding properties similar to those of frataxin [56].

1.12. Frataxin

Bacterial frataxin (CyaY) is an acidic protein that can bind and deliver iron ions. The eukaryotic ortholog of CyaY, frataxin, is well-known for its pivotal function in regulating iron homeostasis in mitochondria [57,58], even though the exact physiological role of this protein is in debate. Recently, however, evidence has been accumulating indicating that CyaY/frataxin is an essential component for Fe–S cluster biosynthesis [18,59]. In particular, it was reported that CyaY/frataxin can form a ternary complex with IscU/Isu1 and IscS/Nfs1 [41,60–63], suggesting that CyaY acts as an iron-chaperone that delivers iron ions to the IscU–IscS complex. However, it was also proposed that CyaY functions as a repressor regulating the iron–sulfur cluster assembly on IscU [40,41].

1.13. IscS

The novel PLP-dependent cysteine desulfurase (IscS) was first identified from a *nifS*-deleted strain of *A. vinelandii* as part of the ISC system [30]. IscS catalyzes the conversion of Cys to Ala. This enzymatic reaction generates a sulfur atom that is picked up by the conserved C328 residue and transferred subsequently to IscU [64] or other proteins, for example, ThiS, which plays an essential role with ThiI in the synthesis of thiamine [65,66]. In addition, sulfur transfer mediated by IscS and ThiI is required for tRNA modification [67]. Homodimeric IscS has been shown to bind to two IscU molecules, either as the apoprotein [61] or as the IscU:[2Fe–2S] complex [68] (see below for details).

1.14. IscU as a hub protein for Fe–S cluster biogenesis

IscU interacts with various protein components to ensure assembly and transfer of Fe–S clusters (Fig. 2). To date, IscU has been shown to interact with IscS [61], HscA and HscB [69], IscX [70], CyaY [41,71,72], IscA [46], and Fdx [45,71]. In addition, holo-IscU donates a cluster to the repressor protein (IscR) [37]. This tangled, yet regulated, web of interactions is physiologically important to safely manipulate iron and sulfur ions whose uncontrolled release would be harmful to the cell and might produce complex and rather unstable Fe–S clusters [8].

In an early study of *Thermotoga maritima* IscU, it was suggested that the protein exists as a molten globule [73]. Subsequently, it was proposed that IscU is an “orphan protein” that requires interaction with a partner in order to be structured [74]. The early structural studies of IscU were of its complex with Zn^{2+} (Table 1). These structures showed that the three conserved cysteine residues (C37, C63, and C106) coordinate the metal, but the fourth ligand was reported differently in X-ray structures as the conserved D39 [75,76] or in an NMR structure as the conserved H105 [77]. The X-ray structures of [2Fe–2S]:IscU [78] and the [2Fe–2S]:IscU–IscS complex [68] showed the ligands as C37, C63, H105, and C106 (in the *E. coli* numbering system); however, the more

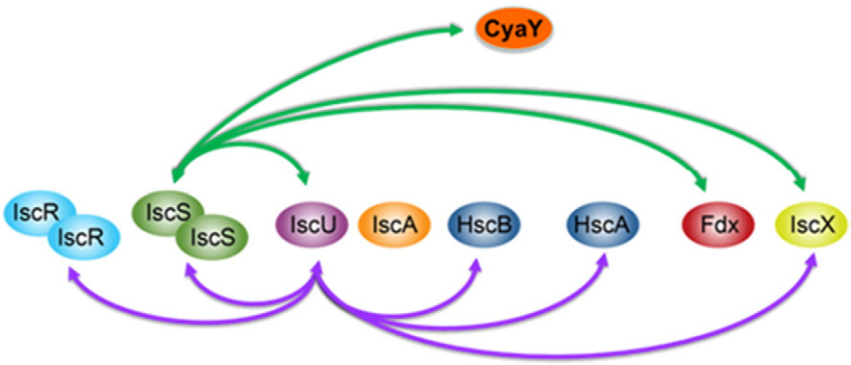

Fig. 2. Network of protein–protein interactions involving IscU (*purple*) and IscS (*green*).

stable IscU variant D39A was used in both studies, which eliminated this potential ligand.

1.15. Role of the cysteine desulfurase (IscS) in catalyzing Fe–S cluster assembly

In the Fe–S cluster assembly mechanism, IscS not only catalyzes sulfur production and transfer, but also acts as a supporting platform on which protein components join and collaborate. Recent X-ray structures of IscS–IscU complexes have provided insights regarding the complex formation and sulfur transfer mechanism. One study showed that the N-terminal region of IscU, which is flexible in its apo-state, forms an α-helical structure and constructs a major binding site for IscS [61]. In addition, C328 of IscS, the essential residue for sulfur withdrawal and transfer, appeared to be capable of acting as a transient ligand for the [2Fe–2S] cluster assembled on IscU; this cysteine residue resides in the flexible loop that can travel a distance of more than 14 Å between the presumed sites of sulfur generation and delivery [68].

In addition, IscS accommodates the binding of other proteins, Fdx, IscX, and CyaY (Fig. 2). Prischi et al. showed by SAXS and NMR spectroscopy that CyaY binds to IscS on which IscU is bound, and suppresses Fe–S cluster assembly [41]. Kim et al. found that the binding of Fdx, IscX, and CyaY to IscS are each mutually exclusive [71], and this finding was confirmed by Yan et al. [79]. The binding interface on IscS for the three proteins appears to involve interactions with a positively-charged patch that includes R220, R223, and R225.

1.16. Roles of the chaperone (HscA) and co-chaperone (HscB) in catalyzing Fe–S cluster transfer

Prior studies have indicated that, whereas IscU can transfer Fe–S clusters by itself, HscA and HscB significantly enhance the rate of cluster transfer [45] in an entirely ATP-dependent reaction [69,80]. Formation of the HscA–IscU–HscB ternary complex synergistically enhances the ATPase activity of HscA by nearly 1000-fold [69], which in turn regulates the lifetime of the HscA–IscU:[2Fe–2S]–HscB complex and the ensuing rate of cluster transfer [80]. The importance of HscA and HscB in chaperoning Fe–S cluster transfer was illustrated by Tokumoto et al. [36] who inactivated either *hscA* or *hscB* and observed considerably decreased cellular growth rates and activities of Fe–S proteins, including succinate dehydrogenase.

1.16.1. Kinetics of HscA in comparison to that of DnaK, the canonical E. coli Hsp70 chaperone

Vickery and coworkers [81,82] identified a novel 66 kDa heat shock protein (Hsp; HscA), whose amino acid sequence displayed 41% identity with DnaK, *E. coli*'s canonical Hsp70 chaperone involved in protein homeostasis (proteostasis) [83]. Further biochemical analyses, however, indicated that HscA expression was not induced by heat shock [81], nor could the protein interact functionally with components of the DnaK/DnaJ/GrpE molecular chaperone system [84]. Initial studies of HscA characterized the kinetics of ATP binding and hydrolysis and revealed that HscA exhibits low basal ATPase activity ($0.10\ min^{-1}$) [85] similar to other Hsp70s [86]; yet, HscA failed to bind to an ATP affinity column [81]. This weak interaction with ATP was further explored by stopped-flow fluorescence. The resultant K_d^{ATP} (26 μM) [85], which was nearly four orders of magnitude larger than that for DnaK (~0.002 μM) [87], explained the failed attempt to capture HscA via ATP affinity columns. Unlike other members of the Hsp70 family [83,86], HscA does not require a nucleotide exchange factor (NEF) to reset its ATPase cycle [84,85]. This apparently is a consequence of HscA's high rates of ADP and ADP-P_i dissociation. Moreover, extensive kinetic analyses, which indicated that ATP hydrolysis occurs at a rate $>10^3$-fold slower than exchange of ADP for ATP, demonstrated that HscA is not subjected to co-chaperone-mediated regulation of ATP hydrolysis and exchange, as are other Hsp70s including DnaK [83,85]. Kinetic values for HscA and DnaK are summarized in Table 2.

Despite the wealth of kinetic information, the structural basis for these unique features of nucleotide association and dissociation have remained unresolved, for no atomic-level information about HscA's nucleotide-binding domain has been reported. Based on the nucleotide dissociation from Hsp70–NEF complexes, it has been hypothesized [88] that the structure of HscA's NBD will be similar to that of DnaK bound to its NEF (GrpE; PDB 1dkg), in which domain IIB is rotated by 14° relative to its position in the ADP-Hsc70 crystal structure thereby facilitating dissociation of ADP-P_i from DnaK [89].

1.16.2. Interactions between HscA and its co-chaperone HscB

To investigate the interactions between HscA and its Hsp40 co-chaperone, HscB, Silberg et al. [51] utilized surface plasmon resonance

Table 2
Comparison of the kinetic parameters for the ATPase cycles of HscA (*E. coli*'s specialized Hsp70-type chaperone for Fe–S cluster biosynthesis) and DnaK (*E. coli*'s canonical Hsp70 chaperone).[a]

Parameter	HscA	DnaK
K_d^{ATP}	26 μM	0.001–0.007 μM [154]
k_a^{ATP}	$4.24 \times 10^4\ M^{-1}\ s^{-1}$	$8 \times 10^6\ M^{-1}\ s^{-1}$ [155]
k_d^{ATP}	$1\ s^{-1}$	$0.008–0.056\ s^{-1}$ [155]
K_m^{ATP}	13 μM	0.02 μM [154]
K_d^{ADP}	90 μM	0.025–0.13 μM [156]
k_a^{ADP}	$7 \times 10^5\ M^{-1}\ s^{-1}$	$1 \times 10^6\ M^{-1}\ s^{-1}$ [156]
k_d^{ADP}	$60\ s^{-1}$	$0.006–0.035\ s^{-1}$ [154]
k_{hyd}	$0.0014\ s^{-1}$	$0.0003–0.0014\ s^{-1}$ [157]
k_{conf}	$0.10\ s^{-1}$	$0.67–1.5\ s^{-1}$ [156]
NEF[b]	None	GrpE [89]

[a] Kinetic data pertaining to HscA were derived from reference [85], whereas sources of DnaK data are listed adjacent to the respective parameter values.
[b] Nucleic acid exchange factor.

(SPR) to determine that HscB interacts primarily with the ATP-bound form of HscA. Binding to HscB stimulated HscA's ATPase activity 5–10 fold [84], a factor similar to those for other Hsp70–Hsp40 pairs, and the HscA–HscB interaction was hypothesized to involve HscA's NBD and HscB's conserved J-domain (JD) [88]. Supporting this hypothesis, Kim et al. recently demonstrated that the J-domain of HscB, which contains the highly conserved His-Pro-Asp (HPD) motif of Hsp40s, binds to HscA in the presence of ATP (Fig. 3).

1.16.3. Interactions between HscA and its substrate IscU

Unlike other Hsp70s that bind to a variety of unfolded hydrophobic polypeptide sequences, HscA was found to exclusively recognize hydrophobic peptides containing a central Pro-Pro motif [90]. The minimal binding site on IscU was subsequently determined to encompass a highly conserved Leu-Pro-Pro-Val-Lys sequence (IscU ^{99}LPPVK^{103}) [90]. Binding of IscU stimulated HscA's ATPase activity 6–8 fold with half-maximal stimulation (K_m^{IscU}) occurring at 30 μM [51,91], whereas a synthetic IscU peptide corresponding to residues ^{98}ELPPVKIHC^{106} elicited nearly identical results (4-fold stimulation and $K_m^{IscU\ peptide} = 27$ μM) [92]. Subsequently, Cupp-Vickery et al. [93] solved the crystal structure of HscA SBD bound to ELPPVKIHC at a resolution of 1.95 Å, in which the overall structure resembled DnaK SBD bound to the peptide NRLLLTG [94], yet the orientation of ELPPVKIHC was reversed with respect to that of DnaK's substrate peptide, which was predicted by fluorescence quenching experiments [95].

Alanine scanning mutagenesis determined that P101 is essential for both binding to HscA and concomitant ATPase stimulation [92]. Confirming these results, the residue corresponding to P101 of IscU was found to be completely buried by hydrophobic interactions in the crystal structure of the HscASBD–peptide complex [93].

The above results were confirmed by SPR studies in which HscB significantly enhanced IscU's binding affinity to ATP–HscA ($K_d^{IscU} = 37$ μM alone; $K_d^{IscU–HscB} = 0.10$ μM and $K_m^{IscU–HscB} = 2$ μM in the presence of HscB) whereas HscB had no effect on the affinity of ELPPVKIHC [51]. Moreover, HscB and IscU synergistically enhanced HscA's ATPase activity by nearly 1000-fold [69]; yet equivalent amounts of HscB and ELPPVKIHC only reached 15-fold stimulation [90]. Such finely tuned synergy reflects the delicate balance with which HscB–IscU–HscA interactions modulate efficient and rapid transfer of Fe–S clusters to apoproteins.

2. Experimental approaches

It has been difficult to obtain information about the complexes of ISC proteins because they are weak and involve dynamic interactions. As a result, many complexes have resisted crystallization. We and others have turned to NMR spectroscopy and small-angle X-ray scattering (SAXS) to study the interactions of these proteins. Chemical crosslinking has also been useful in confirming information from NMR and SAXS.

In the context of our work, we have identified and characterized protein–protein interactions within the ISC-assembly system using several NMR spectroscopic approaches. The simplest experiments involve recording 2D ^{1}H–^{15}N HSQC (heteronuclear single-quantum correlation) spectra of protein mixtures in which a protein labeled with an NMR active isotope (e.g. ^{15}N) is mixed with an NMR "invisible" protein lacking special labeling. The formation of complexes can be rapidly identified by monitoring perturbations in the peaks of 2D ^{1}H–^{15}N HSQC spectra upon mixing the proteins. Because the complex tumbles more slowly in solution than the labeled protein alone, formation of a complex usually results in a broadening of the peaks in the NMR spectrum of the isotopically labeled protein. The binding interface of a protein–protein interaction typically can be determined from the large chemical shift perturbations that occur at residues localized at the binding interface. In most cases, these experiments can be utilized without the need for intricate isotopic labeling schemes or more complicated NMR experiments. Simple NMR experiments such as the 2D ^{1}H–^{15}N HSQC have provided rapid atomic level insight into these challenging to study ISC protein–protein complexes.

Solution SAXS, which provides low-resolution insight into molecular shapes, is a highly complementary approach to NMR for studying proteins and protein–protein complexes. The simplest types of information afforded from SAXS experiments are the radius of gyration (R_g) and the molecular mass of the protein or protein–protein complex. The formation of complexes or oligomerization can usually be quickly identified by an increase in the R_g or molecular mass. SAXS experiments can also be used to generate low-resolution molecular shape models. Protein binding interactions can be identified from a change in molecular shape resulting from complex formation. For example, the expansion of the end-to-end distance (D_{max}) in a protein's molecular shape upon complex formation can be used to help identify the binding site if the structures of the subunits are known. It is important to note that, given the low resolution of SAXS, several degenerate orientations of

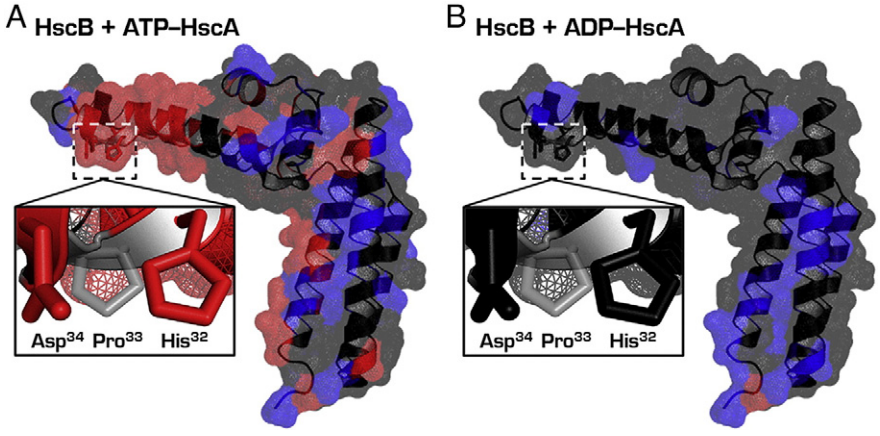

Fig. 3. Results from 2D ^{1}H–^{15}N HSQC experiments that identified the nucleotide-dependent HscA binding surface upon HscB. [U–^{15}N]–HscB was mixed with 3 molar equivalents of unlabeled HscA(T212V), which included a mutation that rendered the protein unable to cleave ATP, in the presence of either ATP (A) or ADP (B). Detailed NMR chemical shift perturbation data can be found in. Depicted here is the structure of HscB (PDB 1fpo; [149]) with ATP- or ADP-HscA-induced $^{1}H^{N}$–$^{15}N^{H}$ chemical shift perturbations ($\Delta\delta_{NH}$) mapped onto the surface of HscB. In *red* are [U–^{15}N]-HscB $^{1}H^{N}$–$^{15}N^{H}$ signals that could not be followed due to severe line broadening; in *blue* are signals with $\Delta\delta_{NH} > 0.01$ ppm; and in *black* are signals with $\Delta\delta_{NH} < 0.01$ ppm, or signals that were unassigned (e.g. proline residues). The insets in both (A) and (B) indicate a region of the J-domain that contains the highly conserved His-Pro-Asp (HPD) motif (HscB numbering: ^{32}HPD^{34}). Residues have been color coded as above, except that Pro^{33} was colored *gray* to indicate its lack of NMR signal in the 2D ^{1}H–^{15}N HSQC experiment.

the protein components can satisfy the molecular shape of the complex. These degeneracies can be broken by adding additional information from complementary experiments such as NMR.

The global structural information afforded by SAXS combined with the atomic-level insight provided by NMR makes them a powerful combination for studying protein–protein complexes [96,97]. Information obtained from NMR and SAXS is easily combined because all experiments can be carried out under identical solution conditions. Low-resolution molecular models of complexes can be built from NMR/SAXS data if the structures of the individual subunits are known. Here, the binding interfaces determined by NMR can be used to piece together structural models that satisfy the molecular shape obtained from SAXS. This approach has been used for complexes of proteins in the ISC operon for which structures are known [41,70,79].

3. Recent results from our laboratory

3.1. Metamorphic property of IscU

IscU appears to accommodate its wide variety of interactions by an unusual, intrinsic conformational flexibility [39]. Our NMR investigations have revealed that IscU populates two conformational states under physiological conditions that interconvert on the order of 1 s^{-1} [98]. One of these states (S-state) is more structured and the other (D-state) is more dynamic, but not unfolded (Fig. 4) [98,99]. We found that the conformational transition between the two states involves *cis*/*trans* isomerization of two peptidyl–prolyl peptide bonds, both of which are *trans* in the S-state of IscU, and both are in the higher energy *cis* configuration in the D-state of IscU (Fig. 4) [99]. Notably, this observation indicates that the D-state of IscU differs from a fully-unfolded state, which should contain peptidyl peptide bonds primarily in the *trans* configuration.

The conformational equilibrium of IscU is maintained with a subtle balance; this is attributed to the necessity of IscU to efficiently interconvert between ordered and dynamic states [39]. The conformational transition of IscU has been mimicked and further characterized under various conditions. For example, the binding of Zn^{2+} [77], Fe^{2+} [100], or [2Fe–2S] [78] stabilizes the S-state (Figs. 5A, B). We also found that the conformational equilibrium of IscU could be perturbed by introducing single-amino acid substitutions: e.g. D39A, D39I, D39V, N90A, S107A, and E111A stabilize the S-state, whereas K89A and N90D stabilize the D-state of IscU [100,101]. We were able to determine the 3D NMR solution structure of the S-state of IscU in the presence of ~20% of the D-state (Fig. 5C) [101]. The least ordered regions of IscU were found to include the loops containing the cluster ligands. Because of its dynamics, determination of the 3D structure of the D-state has proved much more challenging and constitutes an ongoing effort in our laboratory. We also determined the NMR solution structure of IscU(D39A) and, as expected, found it to be more ordered than that of wild-type IscU [101].

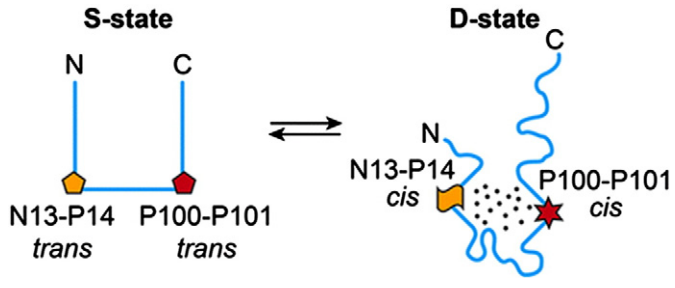

Fig. 4. Schematic representation of conformational equilibrium of IscU. In its apo-state, IscU exists as a metamorphic protein, showing two different conformations; the more structured state (S-state) and the more dynamic state (D-state). This conformational transition is correlated with *cis*/*trans* isomerization of two peptidyl–prolyl peptide bonds, N13–P14 and P100–P101.
Adapted from [39].

In addition, the S ⇄ D conformational equilibrium of IscU depends on temperature and pH. We observed that the S-state of IscU is most highly populated at 25 °C and that increasing or decreasing the temperature destabilizes the S-state; only the D-state of IscU was observed at 45 °C [39,99]. Intriguingly, IscU manifests effects analogous to cold denaturation well above 0 °C, again reflecting the delicate balance in maintaining its metamorphic nature [39,102]. The S ⇄ D conformational equilibrium of IscU is pH-dependent with the S-state maximally populated at pH ~ 8 and transitions to the D-state at low and high pH [103]. We found that the conformational transition at low pH can be ascribed to differences in the pK_a values of the two conserved histidine residues (H10 and H105) in the S- and D-states and have suggested that the conformational transition at high pH similarly results from differences in the pK_a values of other residues, most likely one or more cysteines, in the S- and D-states.

Most interestingly, we found that the different proteins known to bind IscU prefer either the S- or D-state. The D-state is preferred by IscS [100] and HscA [104], whereas the S-state is preferred by HscB [98,104] and IscX [70].

3.2. Mechanism of Fe–S cluster assembly

Recent studies from our laboratory have yielded separate pieces to the puzzle of Fe–S cluster assembly. We discovered that reduced Fdx binds to IscS and becomes oxidized only in the presence of L-cysteine and only if C328 of IscS is intact [71]. In addition, we found that reduced Fdx serves as a reductant for in vitro cluster assembly [71]. These results suggested that cluster assembly involves the generation of a disulfide radical, possibly located on C328. Another piece to the puzzle was our finding that the binding of Fdx and IscU to IscS is mutually exclusive [71]. NMR studies showed that IscU's site of interaction with IscX (Fig. 6) [70] is different from its site of interaction with IscS [61] and that the IscX–IscU interaction is stronger when IscX contains bound Fe^{2+} [70]. In addition, IscX appears to interact more strongly with Fe^{2+} than with Fe^{3+}. These results suggested that IscX is, in fact, the iron donor for cluster assembly and that the iron ion is passed to IscU when it becomes oxidized. Finally, we found that IscX inhibits the cysteine desulfurase activity of IscS by forming a ternary complex with IscU, as identified by NMR and SAXS (Fig. 7) [70]. This mechanism of inhibition is distinct from that of CyaY, which inhibits IscS by displacing both IscU and Fdx [71]. By putting these clues together, we devised a detailed working mechanism for Fe–S cluster assembly (Fig. 8) [70]. The cycle starts with the binding of reduced Fdx to IscS, which displaces IscX from IscS and activates its cysteine desulfurase activity. Conversion of Cys to Ala generates S^0, which is transferred to C328 and reduced by Fdx to a disulfide radical. Next IscU binds to IscS and competes off oxidized Fdx. Fe^{2+}:IscX interacts with IscU as the sulfur radical is transferred to a cysteine of IscU, and its bound Fe^{2+} is oxidized to Fe^{3+} and transferred to IscU as $S^{\bullet-}$ is reduced to S^{2-}. IscX can then bind to IscS to inhibit cysteine desulfurase activity until it is displaced by reduced Fdx to initiate the second cycle. This second cycle involves the conversion of a second Cys to Ala, conversion of the S^0 formed to $S^{\bullet-}$ by oxidation of Fdx, delivery of a second iron ion from IscX:Fe^{2+}, reduction of $S^{\bullet-}$ and incorporation of a second Fe^{3+} to form IscU:[2Fe–2S].

3.3. Mechanism of Fe–S cluster transfer

Upon assembly of an Fe–S cluster on IscU, cluster transfer takes place through the recruitment of additional protein chaperones (HscA and HscB). These two proteins facilitate Fe–S cluster transfer through the well-known ATP-dependent Hsp70/Hsp40 cycle [88]. We began by

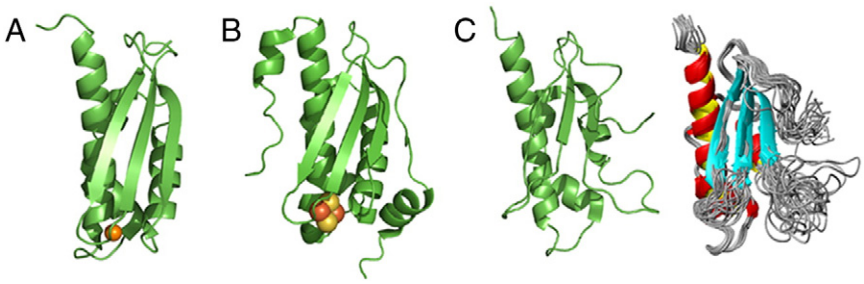

Fig. 5. Structural models of IscU in its S-state. (A) NMR solution structure of *Haemophilus influenzae* Zn-bound IscU (PDB 1r9p; [77]). Zn is shown as an *orange* sphere. Note that the disordered N-terminal region (M1–L20) is not shown here. (B) X-ray crystal structure of *Aquifex aeolicus* [2Fe–2S]-bound IscU (PDB 2z7e; [78]). The structure is trimeric with only one molecule in the asymmetric unit containing the [2Fe–2S] cluster (shown as spheres). (C) NMR solution structure of *E. coli* apo-IscU (PDB 2l4x; [101]). (Left) Representative structure. (Right) Ensemble of the 20 lowest-energy structural models.

investigating the interaction between HscB and IscU. Through a combination of NMR spectroscopy, circular dichroism (CD) spectroscopy, isothermal titration calorimetry (ITC), and site-directed mutagenesis, we found that HscB uses three conserved hydrophobic residues (L92, M93, and F153) to form a hydrophobic core when associating with IscU [105,106]. Conversely, we identified two hydrophobic residues of IscU (M31 and V40) at the HscB interaction site [98]. Notably, we further showed that HscB only targets the S-state of IscU [104], which is consistent with previous speculations that the S-state of IscU sustains the assembled Fe–S cluster until its transfer, and that HscB guides the Fe–S cluster-bound IscU to HscA [51].

Next, we investigated the binary interactions between HscA and IscU or HscB, and the subsequent ternary complex with HscB. As noted above, prior information about the structure of the HscA–IscU complex came from the X-ray crystal structure of the complex between the substrate binding domain (SBD) of HscA and the IscU peptide ^{98}ELPPVKIHC^{106} [93]. This study showed that the peptide bound to the SBD adopts an extended conformation, suggesting that IscU needs to undergo a significant conformational change to accommodate this non-native conformation. We confirmed this speculation by NMR spectroscopy, which revealed that HscA, in its apo- or ADP-bound state, binds to and stabilizes the D-state of IscU, whereas S-state IscU does not interact with HscA regardless of a bound-nucleotide [104]. Because the D-state IscU does not bind metal ions (or a cluster), this result suggests that the HscA-induced S → D conversion serves to release the cluster to an acceptor apoprotein. When HscA contains bound ATP, this interaction with IscU fails to occur [104]. Thus, we have postulated that the trigger for the activation of the ATPase activity of HscA in the IscU:[2Fe–2S]–HscB–HscA:ATP complex is the attack of the iron ions of the cluster by one (or more probably two) of the free –SH groups of the acceptor apoprotein [39,104]. The attack of two cysteine side chains would release two of IscU's ligands to the cluster, most probably H105 and C106. This would free up the sequence of IscU that binds to HscA. We have speculated that this change in ligation affects the interaction between IscU and HscB in a way that perturbs the interaction between the HscB and the nucleotide binding domain (NBD) of HscA to activate its ATPase activity [107]. The resulting nucleotide-induced conformational change in HscA converts it to the state that binds IscU, and binding to the D-state of IscU leads to complete release of the cluster to the acceptor protein. This mechanism is illustrated in Fig. 9. One virtue of

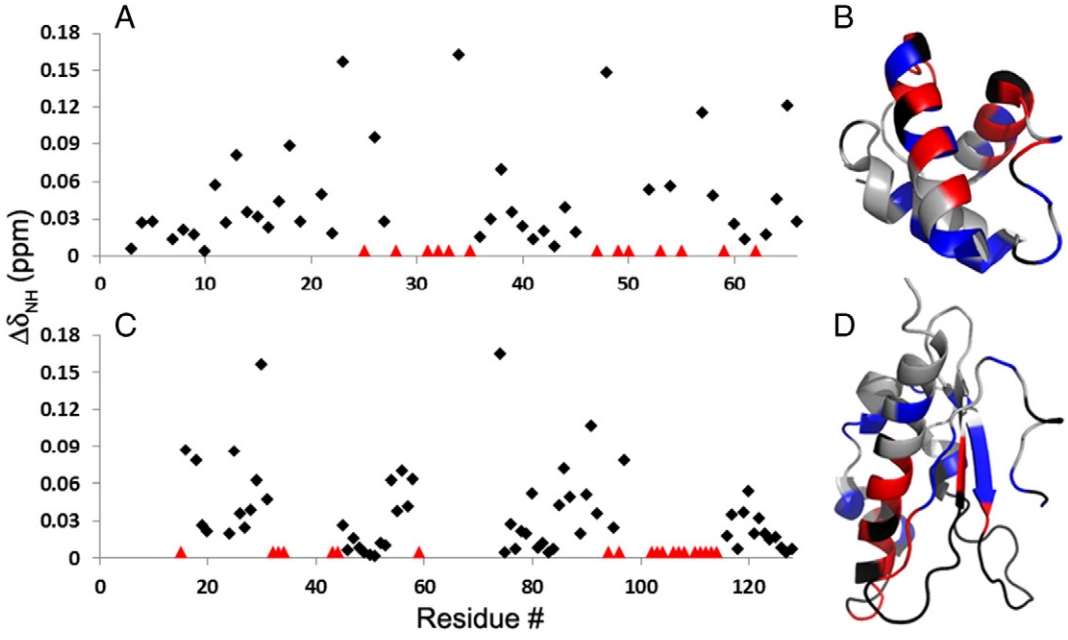

Fig. 6. NMR evidence from 2D ^{1}H–^{15}N HSQC spectra for the surfaces by which IscX and IscU interact. (A) Perturbation of the $^{1}H^{N}$–$^{15}N^{H}$ signals ($\Delta\delta_{NH}$) of [U–^{15}N]–IscX, resulting from the addition of 4 equivalents of IscU. *Red* triangles denote residues whose chemical shift changes could not be followed because of severe line broadening. (B) Results from panel A mapped onto the structure of IscX (PDB 2bzt)[17] with the following color code: *gray*, not affected; *blue*, significantly shifted ($\Delta\delta_{NH} > 0.04$ ppm); *red*, broadened; *black*, not assigned or overlapped. (C) Perturbation of the $^{1}H^{N}$–$^{15}N^{H}$ signals of [U–^{15}N]–IscU resulting from the addition of 4 equivalents IscX. *Red* triangles denote residues whose chemical shift changes could not be followed because of severe line broadening. (D) Results from panel C mapped onto the structure of IscU (PDB 2l4x)[33] with the same color code used for panel B.
Reprinted with permission from [70]. Copyright (2014) American Chemical Society.

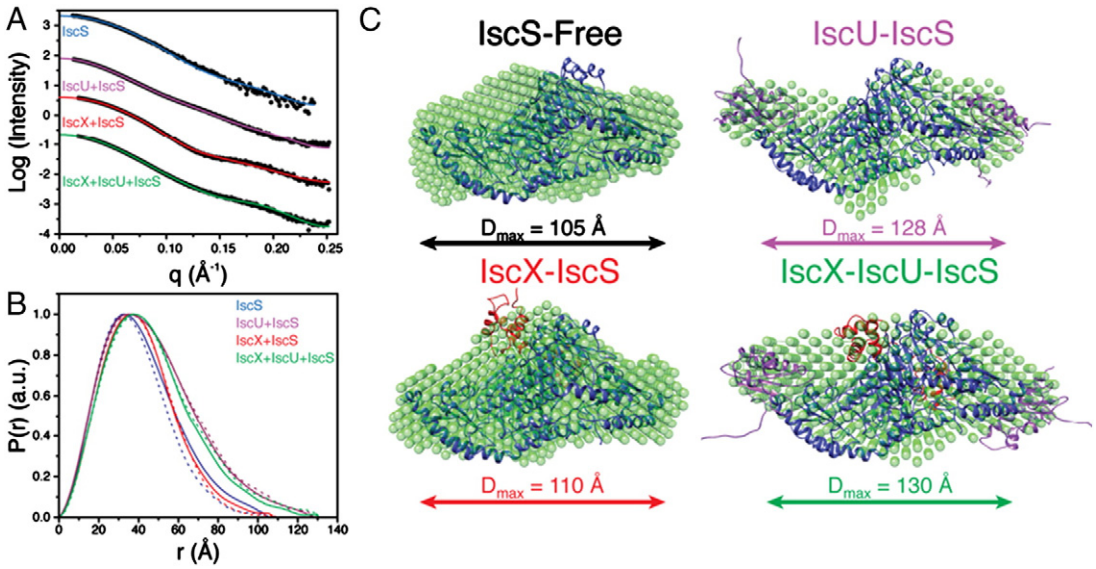

Fig. 7. Structural models from SAXS data. (A) Experimental SAXS data (circles) recorded for IscS (*blue*), IscU + IscS (*purple*), IscX + IscS (*red*), and IscX + IscU + IscS (*green*). Fits of the molecular models for IscS (PDB 1p3w) and those determined from rigid body modeling to experimental SAXS are plotted as solid lines. (B) Pairwise distance distribution functions derived from experimental SAXS data (solid-lines) for IscS (*blue*), IscU + IscS (*purple*), IscX + IscS (*red*), and IscX + IscU + IscS (*green*) compared to those derived from the rigid body modeling derived structures (dashed-lines). (C) Molecular models of IscS (*black*, PDB 1p3w), IscU–IscS (*purple*), IscX–IscS (*red*), and IscX–IscU–IscS (*green*), determined from rigid body modeling simulations. The structures used for each complex component in the rigid body modeling simulations were: IscS (*blue*; PDB 1p3w) [136], IscU (*purple*; PDB 2l4x) [101], and IscX (*red*; PDB 2bzt) [56]. The resulting structures from rigid body modeling are overlaid with ab initio shape models determined from the SAXS data with DAMMIF [158].
Reprinted with permission from [70]. Copyright (2014) American Chemical Society.

the proposed mechanism is that ATP hydrolysis occurs only in the presence of an acceptor protein thus avoiding idle cycles of ATP hydrolysis.

Intriguingly, when probing the interactions between HscA and HscB, Kim et al. identified an HscA interaction site on the C-terminal domain of HscB. This second, less nucleotide-dependent interface (see "Interactions between HscA and its co-chaperone HscB" section above) contained HscB residues (R152, D155, K156, R158, and Q163) [106] that reside near those previously found (R87, L92, L96, R99, E100, and F153) to interact with IscU [98,105,106]. Thus, a model arises in which HscB, via its C-terminal domain, could facilitate interactions between IscU and HscA during Fe–S cluster transfer. Experimental support of such a model, however, will require detailed structural investigations of the elusive ATP:HscA–HscB–IscU complex.

3.4. Ligation pattern of the holo-repressor: IscR:[2Fe–2S]

IscR is the homodimeric [2Fe–2S] transcription factor that regulates expression of more than 40 genes, including the *E. coli isc* operon that encodes IscR itself [37]. This protein targets two different DNA motifs; the cluster-bound IscR is able to recognize both of these DNA sequences, whereas apo-IscR binds to only one motif, indicating that the regulation mechanism of IscR depends on the redox state of a cell and availability of iron and sulfur [108]. In further support of this redox-dependent regulation, a recent study revealed the atypical cluster coordination ligands of IscR. By employing resonance Raman, Mössbauer, and NMR spectroscopy, Fleischhacker et al. [109] showed that one of the cluster ligands of IscR is the histidine residue, H107; the other ligands were earlier

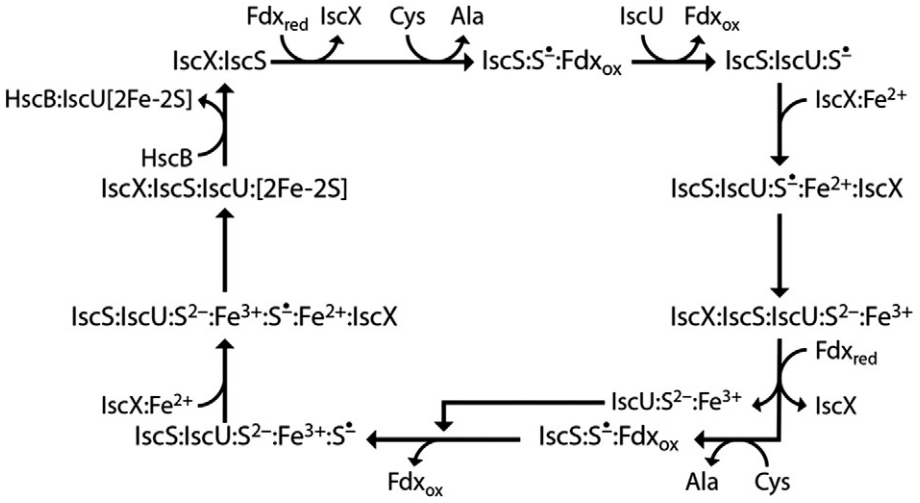

Fig. 8. Proposed mechanism for the ISC Fe–S cluster assembly. In this scheme IscX serves both as the source of Fe^{2+} and as a regulator of cysteine desulfurase (IscS). The species $S^{\bullet}$ is bound to the sulfur of a cysteine residue of either IscS or IscU as indicated, and S^{2-}:Fe^{3+} is bound to a cysteine residue of IscU as Cys–S–Fe–S. Details are provided in the text. Not shown is CyaY, which inhibits Fe–S cluster assembly by binding to IscS and competing off Fdx and IscU.
Reprinted with permission from [70]. Copyright (2014) American Chemical Society.

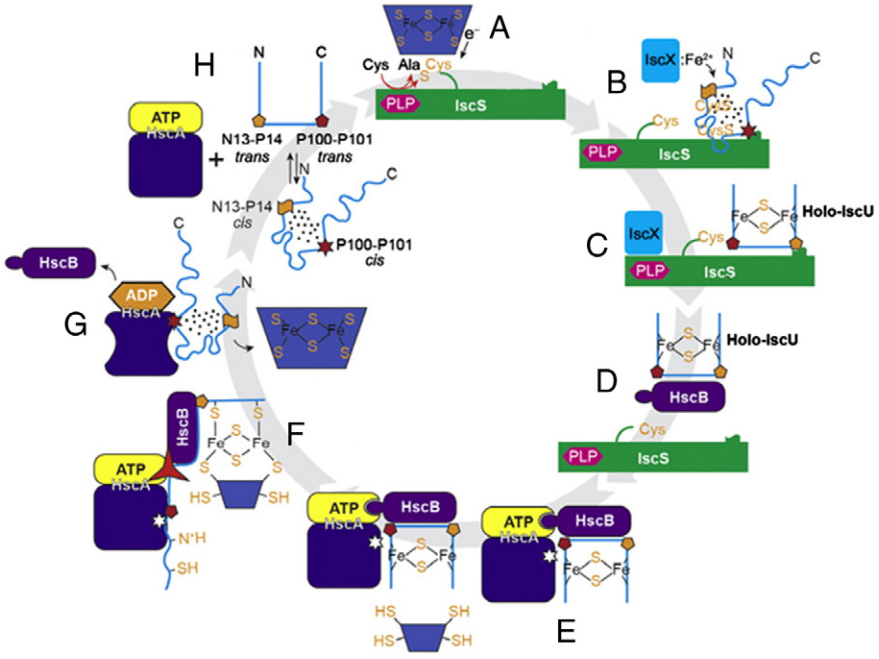

Fig. 9. Schematic representation of the role of the S- and D-states of IscU in Fe–S cluster assembly on IscU and delivery to an acceptor apoprotein. (A) Reduced Fdx donates an electron to reduce the S^0 generated by conversion of Cys to Ala by IscS. (B) The D-state of IscU binds to IscS displacing Fdx, and the sulfur radical is transferred from IscS to IscU and reduced by Fe^{2+} delivered by IscX to S^{2-}. (C) Following the repeat of steps A and B, an assembled [2Fe–2S] cluster is bound to the S-state of IscU. (D) IscU:[2Fe–2S] is transferred from IscS to HscB, which has a higher affinity for the S-state of IscU than does IscS. (E) The J-domain of HscB (round knob) targets the HscB–IscU:[2Fe–2S] complex to the nucleotide binding domain of HscA. (F) The approach of an acceptor apoprotein (blue trapezoid) and subsequent attack of two of its –SH groups on the iron ions of the complex liberates two of the IscU cluster ligands, leading to a conformational change in HscB that activates the ATPase activity of HscA. (G) Cleavage of ATP to ADP leads to conversion of the tense state (T) state of HscA to the relaxed state (R), which binds the D-state of IscU. Conversion of IscU from the S- to the D-state by binding to HscA(ADP), releases the cluster to the acceptor protein, and HscB. (H) Finally, exchange of bound ADP for ATP converts HscA back to the T-state with release of IscU, which resumes its equilibrium between the S- and D-states.
Adapted from [39] on the basis of new results [70]

identified as confirmed to three cysteine residues, C92, C98, and C104 [110]. A variety of spectroscopic data were consistent with a non-cysteinyl ligand to the [2Fe–2S] cluster, and the combination of site-directed mutagenesis and histidine-selective labeling led to the assignment of NMR signals from the fourth ligand to histidine [109].

This non-classical $(Cys)_3(His)_1$ Fe–S cluster ligation scheme is identified in Fe–S proteins that show sensing activities. For example, $(Cys)_3(His)_1$, ligation is found in the yeast Fra2/Grx3 complex, which is responsible for sensing cellular Fe-status [111], and in the outer mitochondrial membrane protein mitoNEET, which has been reported to sense cellular redox states and Fe-status [112,113]. As discussed above, it is probable that IscU utilizes $(Cys)_3(His)_1$ cluster ligation. In the case of IscU, the atypical cluster coordination may serve to reduce the protein's affinity of the cluster so that it is more easily transferred to an acceptor protein. In the case of IscR, reduced affinity may make the protein a better sensor of the availability of Fe–S clusters.

4. Outstanding questions and challenges for future research

One of the most intriguing features to emerge from our studies is the metamorphic property of IscU [98,99] and the fact that partner proteins prefer one state over the other and thereby serve to modulate the structure of IscU and its chemical properties. Switching between the two states is gated by *cis*/*trans* isomerizations of two peptidyl–prolyl peptide bonds [99]. This concerted conversion occurs at a high rate in the absence of external catalysis by a peptidyl–prolyl isomerase. How did such properties evolve, particularly in such an ancient protein system?

Preliminary studies from our laboratory have shown that the S ⇄ D equilibrium of IscU is influenced by temperature and pH. This line of research offers to shed light on the thermodynamic properties of the transition and how it affects the proton affinity of protein side chains.

We have shown that the S- and D-states of IscU interact differentially with partner proteins, with IscS [100] and HscA [104] binding preferentially to the D-state and IscX [70] and HscB [98,104] binding preferentially to the S-state. The mechanisms for these preferences remain to be worked out in terms of three-dimensional models for the binding sites and the groups responsible for specificity. Current X-ray crystal models do not agree with some of the solution NMR results. For example, the structure of the IscS–IscU complex shows IscU in the S-state [61], likely as the result of additives used in crystallization. This interpretation, however, remains controversial [114], and resolution awaits definitive experimentation. The X-ray crystal structure of the complex between the substrate binding domain of HscA and the peptide fragment of IscU that binds to it (ELPPVKIHC) [93] shows the configuration of the P100–P101 peptide bond in the *trans* configuration found in the S-state, rather than the *cis* configuration found in the D-state. We have found that the binding of CyaY and IscU to IscS is mutually exclusive [71]; however, another group has reported the existence of an IscU:CyaY:IscS ternary complex [41]. Further investigation is warranted regarding these discrepancies.

Given HscA's thorough kinetic characterization and unique nucleotide-binding qualities, it is puzzling that its isolated NBD, which hydrolyzes ATP and promotes Fe–S cluster transfer, has not been studied in detail. Moreover, the role of HscA's highly conserved interdomain linker in modulating the NBD's ATPase activity has only recently been analyzed. A prior study in DnaK [115] reported that mutations in the interdomain linker abolished chaperone activity. Additionally, a DnaK NBD variant containing the linker exhibited autoactivated ATP hydrolysis [116], and its site of binding on the NBD was mapped to a conserved region between domains IA and IIA [116–118]. Alderson et al. [119] compared the ATPase activities of isolated HscA NBD ($HscA_{386}$) variants and reported that, when covalently attached ($HscA_{395}$), HscA's interdomain linker stimulated ATPase activity to levels similar to other

Hsp70s. It thus will be of interest to determine how Hsp70s have evolved the ability to activate ATP hydrolysis via their linker (e.g. DnaK [116], Hsc70 [117]), and, if so, has this linker–NBD interface also been conserved across evolution? More importantly, the HscB binding site upon HscA has yet to be characterized at atomic resolution, likely a result of relatively weak binding interactions that resist crystallization. HscB could not stimulate the ATPase activity of HscA variants that lacked the SBD, which suggested that the SBD either directly contacts HscB or indirectly positions the NBD for functional interactions with HscB [119]. Elucidating the HscA–HscB binding interface will be essential to our mechanistic understanding of co-chaperone-mediated stimulation of ATP hydrolysis and Fe–S cluster transfer.

Although we have advanced models for cluster assembly and delivery, many of the steps involved require verification and lack mechanistic detail. For example, the nature of the radical anion formed on IscS, which occurs by reduction of Fdx accompanied by conversion of Cys to Ala, remains to be determined. Our assumption that it is a disulfide radical anion on C328 of IscS awaits experimental validation. Another question revolves around the possible role of D39 of IscU in cluster assembly [68]. D39 is highly conserved, and its mutation to Ala has phenotypic consequences [43,120,121]. We have shown that cluster stabilization in the D39A variant can be explained by its stabilization of the S-state of IscU [100], but D39 may play additional functional roles. The actual steps in cluster delivery to an acceptor apoprotein remain speculative. We have postulated that the trigger is attack by one, or more likely two, cysteinyl sulfhydryl groups of the acceptor protein on the iron ions of the cluster bound to IscU [39]. This attack would release IscU ligands, probably H105 and C106, leading to a conformational change resulting in activation of the ATPase activity of HscA. Experimental trapping of this postulated intermediate would greatly strengthen this case.

The role of IscA is still in limbo. IscA has been shown to bind Fe^{2+} and Fe^{3+} [122] and Cu^{+} [123]. Various functions have been ascribed to IscA, including iron delivery [48], cluster acceptance and delivery [124], and assembly or maturation of [4Fe–4S] centers [125,126]. IscA (107 aa residues) and IscX (66 aa residues) exhibit 18% sequence identity and may have arisen by gene duplication. IscX lacks the HESB domain with its conserved CGCG sequence present in all IscA proteins [127].

The ISC machinery is capable of producing both [2Fe–2S] and [4Fe–4S] clusters. The way in which the ratio of the two cluster types is regulated remains to be discovered. Also, we have no structural model yet for a [4Fe–4S] cluster bound to IscU. In addition, it is not known whether [4Fe–4S] clusters form only through the fusion of two [2Fe–2S] clusters.

It appears that part of what has been learned with the *E. coli* ISC system will be relevant to the Fe–S cluster assembly and delivery machinery of other organisms. We have shown, for example, that the human mitochondrial scaffold protein (ISCU) has metamorphic properties similar to that of *E. coli* IscU and that the human J-protein (HSC20) binds preferentially to the S-state of ISCU, whereas the cysteine desulfurase (NFS1) and Hsp70-type chaperone (mtHSP70) bind preferentially to the D-state of IscU [128]. Major differences between the bacterial and eukaryotic Fe–S cluster assembly systems are the presence of an accessory protein (ISD11) [129–131] as an essential part of the eukaryotic cysteine desulfurase (NFS1) and the fact that frataxin (FRDA) is a required component [60,132,133], rather than an inhibitor [134]. It appears that there is no homolog of IscX in eukaryotes; frataxin may play the role instead for iron delivery. An important recent finding is that LYR motifs in eukaryotic apo-Fe–S proteins bind to HSC20 and serve to target them for Fe–S cluster delivery; LYR motifs are leading to the identification of many additional genes as coding for Fe–S proteins [135].

Acknowledgements

This work was supported by NIH grant U01 GM94622. This study made use of the National Magnetic Resonance Facility at Madison, which is supported by NIH grant P41GM66326 (NIGMS). Equipment was purchased with funds from the University of Wisconsin-Madison, the NIH (P41RR02301, P41GM66326, S10RR02781, S10RR08438, S10RR023438, S10RR025062, S10RR029220), the NSF (DMB-8415048, OIA-9977486, BIR-9214394), and the USDA. J.R.B. was supported by a Ruth L. Kirschstein National Research Service Award (F32 GM110939).

References

[1] H. Beinert, A tribute to sulfur, Eur. J. Biochem. 267 (2000) 5657–5664.
[2] G. Wachtershauser, Groundworks for an evolutionary biochemistry: the iron–sulphur world, Prog. Biophys. Mol. Biol. 58 (1992) 85–201.
[3] G. Wachtershauser, Origin of life. Life as we don't know it, Science 289 (2000) 1307–1308.
[4] C. Huber, G. Wachtershauser, Peptides by activation of amino acids with CO on (Ni, Fe)S surfaces: implications for the origin of life, Science 281 (1998) 670–672.
[5] G.D. Cody, N.Z. Boctor, T.R. Filley, R.M. Hazen, J.H. Scott, A. Sharma, H.S. Yoder Jr., Primordial carbonylated iron–sulfur compounds and the synthesis of pyruvate, Science 289 (2000) 1337–1340.
[6] C. Huber, G. Wachtershauser, Activated acetic acid by carbon fixation on (Fe, Ni)S under primordial conditions, Science 276 (1997) 245–247.
[7] H. Beinert, Iron–sulfur proteins: ancient structures, still full of surprises, J. Biol. Inorg. Chem. 5 (2000) 2–15.
[8] H. Beinert, R.H. Holm, E. Munck, Iron–sulfur clusters: nature's modular, multipurpose structures, Science 277 (1997) 653–659.
[9] K. Tagawa, D.I. Arnon, Ferredoxins as electron carriers in photosynthesis and in the biological production and consumption of hydrogen gas, Nature 195 (1962) 537–543.
[10] D.C. Johnson, D.R. Dean, A.D. Smith, M.K. Johnson, Structure, function, and formation of biological iron–sulfur clusters, Annu. Rev. Biochem. 74 (2005) 247–281.
[11] J. Balk, S. Lobreaux, Biogenesis of iron–sulfur proteins in plants, Trends Plant Sci. 10 (2005) 324–331.
[12] J. Rudolf, V. Makrantoni, W.J. Ingledew, M.J. Stark, M.F. White, The DNA repair helicases XPD and FancJ have essential iron–sulfur domains, Mol. Cell 23 (2006) 801–808.
[13] R. Jain, E.S. Vanamee, B.G. Dzikovski, A. Buku, R.E. Johnson, L. Prakash, S. Prakash, A.K. Aggarwal, An iron–sulfur cluster in the polymerase domain of yeast DNA polymerase epsilon, J. Mol. Biol. 426 (2014) 301–308.
[14] S. Klinge, J. Hirst, J.D. Maman, T. Krude, L. Pellegrini, An iron–sulfur domain of the eukaryotic primase is essential for RNA primer synthesis, Nat. Struct. Mol. Biol. 14 (2007) 875–877.
[15] Y. Zhang, H. Li, C. Zhang, X. An, L. Liu, J. Stubbe, M. Huang, Conserved electron donor complex Dre2-Tah18 is required for ribonucleotide reductase metallocofactor assembly and DNA synthesis, Proc. Natl. Acad. Sci. U. S. A. 111 (2014) E1695–E1704.
[16] P.E. Bishop, M.E. Hawkins, R.R. Eady, Nitrogen fixation in molybdenum-deficient continuous culture by a strain of *Azotobacter vinelandii* carrying a deletion of the structural genes for nitrogenase (nifHDK), Biochem. J. 238 (1986) 437–442.
[17] R. Lill, Function and biogenesis of iron–sulphur proteins, Nature 460 (2009) 831–838.
[18] R. Lill, U. Muhlenhoff, Maturation of iron–sulfur proteins in eukaryotes: mechanisms, connected processes, and diseases, Annu. Rev. Biochem. 77 (2008) 669–700.
[19] S.L. Liochev, The role of iron–sulfur clusters in in vivo hydroxyl radical production, Free Radic. Res. 25 (1996) 369–384.
[20] R. Lill, U. Muhlenhoff, Iron–sulfur protein biogenesis in eukaryotes: components and mechanisms, Annu. Rev. Cell Dev. Biol. 22 (2006) 457–486.
[21] R. Lill, B. Hoffmann, S. Molik, A.J. Pierik, N. Rietzschel, O. Stehling, M.A. Uzarska, H. Webert, C. Wilbrecht, U. Muhlenhoff, The role of mitochondria in cellular iron–sulfur protein biogenesis and iron metabolism, Biochim. Biophys. Acta 1823 (2012) 1491–1508.
[22] D.J. Netz, J. Mascarenhas, O. Stehling, A.J. Pierik, R. Lill, Maturation of cytosolic and nuclear iron–sulfur proteins, Trends Cell Biol. 24 (2014) 303–312.
[23] O. Stehling, C. Wilbrecht, R. Lill, Mitochondrial iron–sulfur protein biogenesis and human disease, Biochimie 100 (2014) 61–77.
[24] T.A. Rouault, Biogenesis of iron–sulfur clusters in mammalian cells: new insights and relevance to human disease, Dis. Model. Mech. 5 (2012) 155–164.
[25] T.A. Rouault, W.H. Tong, Iron–sulfur cluster biogenesis and human disease, Trends Genet. 24 (2008) 398–407.
[26] G. Isaya, Mitochondrial iron–sulfur cluster dysfunction in neurodegenerative disease, Front. Pharmacol. 5 (2014) 29.
[27] N. Exner, A.K. Lutz, C. Haass, K.F. Winklhofer, Mitochondrial dysfunction in Parkinson's disease: molecular mechanisms and pathophysiological consequences, EMBO J. 31 (2012) 3038–3062.
[28] L.T. Bennett, M.R. Jacobson, D.R. Dean, Isolation, sequencing, and mutagenesis of the nifF gene encoding flavodoxin from *Azotobacter vinelandii*, J. Biol. Chem. 263 (1988) 1364–1369.
[29] M.R. Jacobson, K.E. Brigle, L.T. Bennett, R.A. Setterquist, M.S. Wilson, V.L. Cash, J. Beynon, W.E. Newton, D.R. Dean, Physical and genetic map of the major nif gene cluster from *Azotobacter vinelandii*, J. Bacteriol. 171 (1989) 1017–1027.
[30] L.M. Zheng, V.L. Cash, D.H. Flint, D.R. Dean, Assembly of iron–sulfur clusters — identification of an iscSUA–hscBA–fdx gene cluster from *Azotobacter vinelandii*, J. Biol. Chem. 273 (1998) 13264–13272.
[31] C. Voisine, Y.C. Cheng, M. Ohlson, B. Schilke, K. Hoff, H. Beinert, J. Marszalek, E.A. Craig, Jac1, a mitochondrial J-type chaperone, is involved in the biogenesis of

Fe/S clusters in *Saccharomyces cerevisiae*, Proc. Natl. Acad. Sci. U. S. A. 98 (2001) 1483–1488.
[32] C. Voisine, B. Schilke, M. Ohlson, H. Beinert, J. Marszalek, E.A. Craig, Role of the mitochondrial Hsp70s, Ssc1 and Ssq1, in the maturation of Yfh1, Mol. Cell. Biol. 20 (2000) 3677–3684.
[33] E.A. Craig, J. Marszalek, A specialized mitochondrial molecular chaperone system: a role in formation of Fe/S centers, Cell. Mol. Life Sci. 59 (2002) 1658–1665.
[34] B. Roche, L. Aussel, B. Ezraty, P. Mandin, B. Py, F. Barras, Iron/sulfur proteins biogenesis in prokaryotes: formation, regulation and diversity, Biochim. Biophys. Acta 1827 (2013) 455–469.
[35] U. Tokumoto, S. Nomura, Y. Minami, H. Mihara, S. Kato, T. Kurihara, N. Esaki, H. Kanazawa, H. Matsubara, Y. Takahashi, Network of protein–protein interactions among iron–sulfur cluster assembly proteins in *Escherichia coli*, J. Biochem. 131 (2002) 713–719.
[36] U. Tokumoto, Y. Takahashi, Genetic analysis of the *isc* operon in *Escherichia coli* involved in the biogenesis of cellular iron–sulfur proteins, J. Biochem. 130 (2001) 63–71.
[37] C.J. Schwartz, J.L. Giel, T. Patschkowski, C. Luther, F.J. Ruzicka, H. Beinert, P.J. Kiley, IscR, an Fe–S cluster-containing transcription factor, represses expression of *Escherichia coli* genes encoding Fe–S cluster assembly proteins, Proc. Natl. Acad. Sci. U. S. A. 98 (2001) 14895–14900.
[38] S. Bandyopadhyay, K. Chandramouli, M.K. Johnson, Iron–sulfur cluster biosynthesis, Biochem. Soc. Trans. 36 (2008) 1112–1119.
[39] J.L. Markley, J.H. Kim, Z. Dai, J.R. Bothe, K. Cai, R.O. Frederick, M. Tonelli, Metamorphic protein IscU alternates conformations in the course of its role as the scaffold protein for iron–sulfur cluster biosynthesis and delivery, FEBS Lett. 587 (2013) 1172–1179.
[40] S. Adinolfi, C. Iannuzzi, F. Prischi, C. Pastore, S. Iametti, S.R. Martin, F. Bonomi, A. Pastore, Bacterial frataxin CyaY is the gatekeeper of iron–sulfur cluster formation catalyzed by IscS, Nat. Struct. Mol. Biol. 16 (2009) 390–396.
[41] F. Prischi, P.V. Konarev, C. Iannuzzi, C. Pastore, S. Adinolfi, S.R. Martin, D.I. Svergun, A. Pastore, Structural bases for the interaction of frataxin with the central components of iron–sulphur cluster assembly, Nat. Commun. 1 (2010) 95.
[42] J.N. Agar, C. Krebs, J. Frazzon, B.H. Huynh, D.R. Dean, M.K. Johnson, IscU as a scaffold for iron–sulfur cluster biosynthesis: sequential assembly of [2Fe–2S] and [4Fe–4S] clusters in IscU, Biochemistry 39 (2000) 7856–7862.
[43] M.C. Unciuleac, K. Chandramouli, S. Naik, S. Mayer, B.H. Huynh, M.K. Johnson, D.R. Dean, *In vitro* activation of apo-aconitase using a [4Fe–4S] cluster-loaded form of the IscU [Fe–S] cluster scaffolding protein, Biochemistry 46 (2007) 6812–6821.
[44] C. Krebs, J.N. Agar, A.D. Smith, J. Frazzon, D.R. Dean, B.H. Huynh, M.K. Johnson, IscA, an alternate scaffold for Fe–S cluster biosynthesis, Biochemistry 40 (2001) 14069–14080.
[45] F. Bonomi, S. Iametti, D. Ta, L.E. Vickery, Multiple turnover transfer of [2Fe2S] clusters by the iron–sulfur cluster assembly scaffold proteins IscU and IscA, J. Biol. Chem. 280 (2005) 29513–29518.
[46] H. Ding, R.J. Clark, Characterization of iron binding in IscA, an ancient iron–sulphur cluster assembly protein, Biochem. J. 379 (2004) 433–440.
[47] H. Ding, R.J. Clark, B. Ding, IscA mediates iron delivery for assembly of iron–sulfur clusters in IscU under the limited accessible free iron conditions, J. Biol. Chem. 279 (2004) 37499–37504.
[48] L.T. Jensen, V.C. Culotta, Role of *Saccharomyces cerevisiae* ISA1 and ISA2 in iron homeostasis, Mol. Cell. Biol. 20 (2000) 3918–3927.
[49] U. Muhlenhoff, M.J. Gerl, B. Flauger, H.M. Pirner, S. Balser, N. Richhardt, R. Lill, J. Stolz, The ISC proteins Isa1 and Isa2 are required for the function but not for the *de novo* synthesis of the Fe/S clusters of biotin synthase in *Saccharomyces cerevisiae*, Eukaryot. Cell 6 (2007) 495–504.
[50] P. Walsh, D. Bursac, Y.C. Law, D. Cyr, T. Lithgow, The J-protein family: modulating protein assembly, disassembly and translocation, EMBO Rep. 5 (2004) 567–571.
[51] J.J. Silberg, T.L. Tapley, K.G. Hoff, L.E. Vickery, Regulation of the HscA ATPase reaction cycle by the co-chaperone HscB and the iron–sulfur cluster assembly protein IscU, J. Biol. Chem. 279 (2004) 53924–53931.
[52] H. Lange, A. Kaut, G. Kispal, R. Lill, A mitochondrial ferredoxin is essential for biogenesis of cellular iron–sulfur proteins, Proc. Natl. Acad. Sci. U. S. A. 97 (2000) 1050–1055.
[53] U. Muhlenhoff, N. Richhardt, J. Gerber, R. Lill, Characterization of iron–sulfur protein assembly in isolated mitochondria. A requirement for ATP, NADH, and reduced iron, J. Biol. Chem. 277 (2002) 29810–29816.
[54] S.P. Wu, G. Wu, K.K. Surerus, J.A. Cowan, Iron–sulfur cluster biosynthesis. Kinetic analysis of [2Fe–2S] cluster transfer from holo ISU to apo Fd: role of redox chemistry and a conserved aspartate, Biochemistry 41 (2002) 8876–8885.
[55] S.S. Mansy, G. Wu, K.K. Surerus, J.A. Cowan, Iron–sulfur cluster biosynthesis. *Thermatoga maritima* IscU is a structured iron–sulfur cluster assembly protein, J. Biol. Chem. 277 (2002) 21397–21404.
[56] C. Pastore, S. Adinolfi, M.A. Huynen, V. Rybin, S. Martin, M. Mayer, B. Bukau, A. Pastore, YfhJ, a molecular adaptor in iron–sulfur cluster formation or a frataxin-like protein? Structure 14 (2006) 857–867.
[57] A.L. Bulteau, H.A. O'Neill, M.C. Kennedy, M. Ikeda-Saito, G. Isaya, L.I. Szweda, Frataxin acts as an iron chaperone protein to modulate mitochondrial aconitase activity, Science 305 (2004) 242–245.
[58] D.C. Radisky, M.C. Babcock, J. Kaplan, The yeast frataxin homologue mediates mitochondrial iron efflux. Evidence for a mitochondrial iron cycle, J. Biol. Chem. 274 (1999) 4497–4499.
[59] T.L. Stemmler, E. Lesuisse, D. Pain, A. Dancis, Frataxin and mitochondrial FeS cluster biogenesis, J. Biol. Chem. 285 (2010) 26737–26743.
[60] S. Schmucker, A. Martelli, F. Colin, A. Page, M. Wattenhofer-Donze, L. Reutenauer, H. Puccio, Mammalian frataxin: an essential function for cellular viability through an interaction with a preformed ISCU/NFS1/ISD11 iron–sulfur assembly complex, Plos One 6 (2011) e16199.
[61] R. Shi, A. Proteau, M. Villarroya, I. Moukadiri, L.H. Zhang, J.F. Trempe, A. Matte, M.E. Armengod, M. Cygler, Structural basis for Fe–S cluster assembly and tRNA thiolation mediated by IscS protein–protein interactions, PLoS Biol. 8 (2010) e1000354.
[62] J. Gerber, U. Muhlenhoff, R. Lill, An interaction between frataxin and Isu1/Nfs1 that is crucial for Fe/S cluster synthesis on Isu1, EMBO Rep. 4 (2003) 906–911.
[63] J.D. Cook, K.C. Kondapalli, S. Rawat, W.C. Childs, Y. Murugesan, A. Dancis, T.L. Stemmler, Molecular details of the yeast frataxin–Isul interaction during mitochondrial Fe–S cluster assembly, Biochemistry 49 (2010) 8756–8765.
[64] H.D. Urbina, J.J. Silberg, K.G. Hoff, L.E. Vickery, Transfer of sulfur from IscS to IscU during Fe/S cluster assembly, J. Biol. Chem. 276 (2001) 44521–44526.
[65] R. Kambampati, C.T. Lauhon, IscS is a sulfurtransferase for the in vitro biosynthesis of 4-thiouridine in *Escherichia coli* tRNA, Biochem 38 (1999) 16561–16568.
[66] C.T. Lauhon, R. Kambampati, The *iscS* gene in *Escherichia coli* is required for the biosynthesis of 4-thiouridine, thiamin, and NAD, J. Biol. Chem. 275 (2000) 20096–20103.
[67] R. Kambampati, C.T. Lauhon, Evidence for the transfer of sulfane sulfur from IscS to ThiI during the in vitro biosynthesis of 4-thiouridine in *Escherichia coli* tRNA, J. Biol. Chem. 275 (2000) 10727–10730.
[68] E.N. Marinoni, J.S. de Oliveira, Y. Nicolet, E.C. Raulfs, P. Amara, D.R. Dean, J.C. Fontecilla-Camps, (IscS–IscU)2 complex structures provide insights into Fe_2S_2 biogenesis and transfer, Angew. Chem. Int. Ed. Engl. 51 (2012) 5439–5442.
[69] K.G. Hoff, J.J. Silberg, L.E. Vickery, Interaction of the iron–sulfur cluster assembly protein IscU with the Hsc66/Hsc20 molecular chaperone system of *Escherichia coli*, Proc. Natl. Acad. Sci. U. S. A. 97 (2000) 7790–7795.
[70] J.H. Kim, J.R. Bothe, R.O. Frederick, J.C. Holder, J.L. Markley, Role of IscX in iron–sulfur cluster biogenesis in *Escherichia coli*, J. Am. Chem. Soc. 136 (2014) 7933–7942.
[71] J.H. Kim, R.O. Frederick, N.M. Reinen, A.T. Troupis, J.L. Markley, [2Fe–2S]-ferredoxin binds directly to cysteine desulfurase and supplies an electron for iron–sulfur cluster assembly but is displaced by the scaffold protein or bacterial frataxin, J. Am. Chem. Soc. 135 (2013) 8117–8120.
[72] G. Layer, S. Ollagnier-de Choudens, Y. Sanakis, M. Fontecave, Iron–sulfur cluster biosynthesis: characterization of *Escherichia coli* CYaY as an iron donor for the assembly of [2Fe–2S] clusters in the scaffold IscU, J. Biol. Chem. 281 (2006) 16256–16263.
[73] I. Bertini, J.A. Cowan, C. Del Bianco, C. Luchinat, S.S. Mansy, *Thermotoga maritima* IscU. Structural characterization and dynamics of a new class of metallochaperone, J. Mol. Biol. 331 (2003) 907–924.
[74] F. Prischi, C. Pastore, M. Carroni, C. Iannuzzi, S. Adinolfi, P. Temussi, A. Pastore, Of the vulnerability of orphan complex proteins: the case study of the *E. coli* IscU and IscS proteins, Prot Express Purific 73 (2010) 161–166.
[75] J. Liu, N. Oganesyan, D.H. Shin, J. Jancarik, H. Yokota, R. Kim, S.H. Kim, Structural characterization of an iron–sulfur cluster assembly protein IscU in a zinc-bound form, Proteins 59 (2005) 875–881.
[76] J. Jeyakanthan, S.P. Kanaujia, K. Sekar, Y. Agari, A. Ebihara, A. Shinkai, S. Kuramitsu, S. Yokoyama, Crystal structure of Iron–sulfur cluster biosynthesis protein IscU (TTHA1736) from *Thermus thermophilus* HB8, 2007., http://dx.doi.org/10.2210/pdb2qq4/pdb.
[77] T.A. Ramelot, J.R. Cort, S. Goldsmith-Fischman, G.J. Kornhaber, R. Xiao, R. Shastry, T.B. Acton, B. Honig, G.T. Montelione, M.A. Kennedy, Solution NMR structure of the iron–sulfur cluster assembly protein U (IscU) with zinc bound at the active site, J. Mol. Biol. 344 (2004) 567–583.
[78] Y. Shimomura, K. Wada, K. Fukuyama, Y. Takahashi, The asymmetric trimeric architecture of [2Fe–2S] IscU: implications for its scaffolding during iron–sulfur cluster biosynthesis, J. Mol. Biol. 383 (2008) 133–143.
[79] R. Yan, P.V. Konarev, C. Iannuzzi, S. Adinolfi, B. Roche, G. Kelly, L. Simon, S.R. Martin, B. Py, F. Barras, D.I. Svergun, A. Pastore, Ferredoxin competes with bacterial frataxin in binding to the desulfurase IscS, J. Biol. Chem. 288 (2013) 24777–24787.
[80] K. Chandramouli, M.K. Johnson, HscA and HscB stimulate [2Fe–2S] cluster transfer from IscU to apoferredoxin in an ATP-dependent reaction, Biochemistry 45 (2006) 11087–11095.
[81] L.E. Vickery, J.J. Silberg, D.T. Ta, Hsc66 and Hsc20, a new heat shock cognate molecular chaperone system from *Escherichia coli*, Protein Sci. 6 (1997) 1047–1056.
[82] B.L. Seaton, L.E. Vickery, A gene encoding a DnaK/hsp70 homolog in *Escherichia coli*, Proc. Natl. Acad. Sci. U. S. A. 91 (1994) 2066–2070.
[83] B. Bukau, J. Weissman, A. Horwich, Molecular chaperones and protein quality control, Cell 125 (2006) 443–451.
[84] J.J. Silberg, K.G. Hoff, L.E. Vickery, The Hsc66–Hsc20 chaperone system in *Escherichia coli*: chaperone activity and interactions with the DnaK–DnaJ–grpE system, J. Bacteriol. 180 (1998) 6617–6624.
[85] J.J. Silberg, L.E. Vickery, Kinetic characterization of the ATPase cycle of the molecular chaperone Hsc66 from *Escherichia coli*, J. Biol. Chem. 275 (2000) 7779–7786.
[86] M.P. Mayer, Hsp70 chaperone dynamics and molecular mechanism, Trends Biochem. Sci. 38 (2013) 507–514.
[87] R. Russell, R. Jordan, R. McMacken, Kinetic characterization of the ATPase cycle of the DnaK molecular chaperone, Biochemistry 37 (1998) 596–607.
[88] L.E. Vickery, J.R. Cupp-Vickery, Molecular chaperones HscA/Ssq1 and HscB/Jac1 and their roles in iron–sulfur protein maturation, Crit. Rev. Biochem. Mol. Biol. 42 (2007) 95–111.
[89] C.J. Harrison, M. Hayer-Hartl, M. Di Liberto, F. Hartl, J. Kuriyan, Crystal structure of the nucleotide exchange factor GrpE bound to the ATPase domain of the molecular chaperone DnaK, Science 276 (1997) 431–435.

[90] K.G. Hoff, D.T. Ta, T.L. Tapley, J.J. Silberg, L.E. Vickery, Hsc66 substrate specificity is directed toward a discrete region of the iron–sulfur cluster template protein IscU, J. Biol. Chem. 277 (2002) 27353–27359.
[91] J.J. Silberg, K.G. Hoff, T.L. Tapley, L.E. Vickery, The Fe/S assembly protein IscU behaves as a substrate for the molecular chaperone Hsc66 from *Escherichia coli*, J. Biol. Chem. 276 (2001) 1696–1700.
[92] K.G. Hoff, J.R. Cupp-Vickery, L.E. Vickery, Contributions of the LPPVK motif of the iron–sulfur template protein IscU to interactions with the Hsc66–Hsc20 chaperone system, J. Biol. Chem. 278 (2003) 37582–37589.
[93] J.R. Cupp-Vickery, J.C. Peterson, D.T. Ta, L.E. Vickery, Crystal structure of the molecular chaperone HscA substrate binding domain complexed with the IscU recognition peptide ELPPVKIHC, J. Mol. Biol. 342 (2004) 1265–1278.
[94] S.Y. Stevens, S. Cai, M. Pellecchia, E.R. Zuiderweg, The solution structure of the bacterial HSP70 chaperone protein domain DnaK(393–507) in complex with the peptide NRLLLTG, Protein Sci. 12 (2003) 2588–2596.
[95] T.L. Tapley, L.E. Vickery, Preferential substrate binding orientation by the molecular chaperone HscA, J. Biol. Chem. 279 (2004) 28435–28442.
[96] F. Gabel, B. Simon, M. Nilges, M. Petoukhov, D. Svergun, M. Sattler, A structure refinement protocol combining NMR residual dipolar couplings and small angle scattering restraints, J. Biomol. NMR 41 (2008) 199–208.
[97] A. Grishaev, J. Wu, J. Trewhella, A. Bax, Refinement of multidomain protein structures by combination of solution small-angle X-ray scattering and NMR data, J. Am. Chem. Soc. 127 (2005) 16621–16628.
[98] J.H. Kim, A.K. Füzéry, M. Tonelli, D.T. Ta, W.M. Westler, L.E. Vickery, J.L. Markley, Structure and dynamics of the iron–sulfur cluster assembly scaffold protein IscU and its interaction with the cochaperone HscB, Biochemistry 48 (2009) 6062–6071.
[99] Z. Dai, M. Tonelli, J.L. Markley, Metamorphic protein IscU changes conformation by *cis–trans* isomerizations of two peptidyl–prolyl peptide bonds, Biochemistry 51 (2012) 9595–9602.
[100] J.H. Kim, M. Tonelli, J.L. Markley, Disordered form of the scaffold protein IscU is the substrate for iron–sulfur cluster assembly on cysteine desulfurase, Proc. Natl. Acad. Sci. U. S. A. 109 (2012) 454–459.
[101] J.H. Kim, M. Tonelli, T. Kim, J.L. Markley, Three-dimensional structure and determinants of stability of the iron–sulfur cluster scaffold protein IscU from *Escherichia coli*, Biochemistry 51 (2012) 5557–5563.
[102] C. Iannuzzi, M. Adrover, R. Puglisi, R. Yan, P.A. Temussi, A. Pastore, The role of zinc in the stability of the marginally stable IscU scaffold protein, Protein Sci. 23 (2014) 1208–1219.
[103] Z. Dai, J.H. Kim, M. Tonelli, I.K. Ali, J.L. Markley, pH-induced conformational change of IscU at low pH correlates with protonation/deprotonation of two conserved histidine residues, Biochemistry 53 (2014) 5290–5297.
[104] J.H. Kim, M. Tonelli, R.O. Frederick, D.C. Chow, J.L. Markley, Specialized Hsp70 chaperone (HscA) binds preferentially to the disordered form, whereas J-protein (HscB) binds preferentially to the structured form of the iron–sulfur cluster scaffold protein (IscU), J. Biol. Chem. 287 (2012) 31406–31413.
[105] A.K. Füzéry, J.J. Oh, D.T. Ta, L.E. Vickery, J.L. Markley, Three hydrophobic amino acids in *Escherichia coli* HscB make the greatest contribution to the stability of the HscB–IscU complex, BMC Biochem. 12 (2011) 3.
[106] A.K. Füzéry, M. Tonelli, D.T. Ta, G. Cornilescu, L.E. Vickery, J.L. Markley, Solution structure of the iron–sulfur cluster cochaperone HscB and its binding surface for the iron–sulfur assembly scaffold protein IscU, Biochemistry 47 (2008) 9394–9404.
[107] J.H. Kim, T.R. Alderson, R.O. Frederick, J.L. Markley, Nucleotide-dependent interactions within a specialized Hsp70/Hsp40 complex involved in Fe–S cluster biogenesis, J. Am. Chem. Soc. 136 (2014) 11586–11589.
[108] A.D. Nesbit, J.L. Giel, J.C. Rose, P.J. Kiley, Sequence-specific binding to a subset of IscR-regulated promoters does not require IscR Fe–S cluster ligation, J. Mol. Biol. 387 (2009) 28–41.
[109] A.S. Fleischhacker, A. Stubna, K.L. Hsueh, Y. Guo, S.J. Teter, J.C. Rose, T.C. Brunold, J.L. Markley, E. Munck, P.J. Kiley, Characterization of the [2Fe–2S] cluster of *Escherichia coli* transcription factor IscR, Biochemistry 51 (2012) 4453–4462.
[110] W.S. Yeo, J.H. Lee, K.C. Lee, J.H. Roe, IscR acts as an activator in response to oxidative stress for the suf operon encoding Fe–S assembly proteins, Mol. Microbiol. 61 (2006) 206–218.
[111] H. Li, D.T. Mapolelo, N.N. Dingra, G. Keller, P.J. Riggs-Gelasco, D.R. Winge, M.K. Johnson, C.E. Outten, Histidine 103 in Fra2 is an iron–sulfur cluster ligand in the [2Fe–2S] Fra2–Grx3 complex and is required for in vivo iron signaling in yeast, J. Biol. Chem. 286 (2011) 867–876.
[112] S.E. Wiley, A.N. Murphy, S.A. Ross, P. van der Geer, J.E. Dixon, MitoNEET is an iron-containing outer mitochondrial membrane protein that regulates oxidative capacity, Proc. Natl. Acad. Sci. U. S. A. 104 (2007) 5318–5323.
[113] M.L. Paddock, S.E. Wiley, H.L. Axelrod, A.E. Cohen, M. Roy, E.C. Abresch, D. Capraro, A.N. Murphy, R. Nechushtai, J.E. Dixon, P.A. Jennings, MitoNEET is a uniquely folded 2Fe 2S outer mitochondrial membrane protein stabilized by pioglitazone, Proc. Natl. Acad. Sci. U. S. A. 104 (2007) 14342–14347.
[114] R. Yan, G. Kelly, A. Pastore, The scaffold protein IscU retains a structured conformation in the FeS cluster assembly complex, Chembiochem 15 (2014) 1682–1686.
[115] W. Han, P. Christen, Mutations in the interdomain linker region of DnaK abolish the chaperone action of the DnaK/DnaJ/GrpE system, FEBS Lett. 497 (2001) 55–58.
[116] J.F. Swain, G. Dinler, R. Sivendran, D.L. Montgomery, M. Stotz, L.M. Gierasch, Hsp70 chaperone ligands control domain association via an allosteric mechanism mediated by the interdomain linker, Mol. Cell 26 (2007) 27–39.
[117] J. Jiang, K. Prasad, E.M. Lafer, R. Sousa, Structural basis of interdomain communication in the Hsc70 chaperone, Mol. Cell 20 (2005) 513–524.
[118] A. Zhuravleva, E.M. Clerico, L.M. Gierasch, An interdomain energetic tug-of-war creates the allosterically active state in Hsp70 molecular chaperones, Cell 151 (2012) 1296–1307.
[119] T.R. Alderson, J.H. Kim, K. Cai, R.O. Frederick, M. Tonelli, J.L. Markley, The specialized Hsp70 (HscA) interdomain linker binds to its nucleotide-binding domain and stimulates ATP hydrolysis in both cis and trans configurations, Biochemistry 53 (2014) 7148–7159.
[120] E.C. Raulfs, I.P. O'Carroll, P.C. Dos Santos, M.C. Unciuleac, D.R. Dean, In vivo iron–sulfur cluster formation, Proc. Natl. Acad. Sci. U. S. A. 105 (2008) 8591–8596.
[121] G. Wu, S.S. Mansy, S.P. Wu, K.K. Surerus, M.W. Foster, J.A. Cowan, Characterization of an iron–sulfur cluster assembly protein (ISU1) from *Schizosaccharomyces pombe*, Biochemistry 41 (2002) 5024–5032.
[122] D.T. Mapolelo, B. Zhang, S.G. Naik, B.H. Huynh, M.K. Johnson, Spectroscopic and functional characterization of iron-bound forms of *Azotobacter vinelandii* (Nif) IscA, Biochemistry 51 (2012) 8056–8070.
[123] G. Tan, Z. Cheng, Y. Pang, A.P. Landry, J. Li, J. Lu, H. Ding, Copper binding in IscA inhibits iron–sulfur cluster assembly in *Escherichia coli*, Mol. Microbiol. 93 (2014) 629–644.
[124] D. Vinella, C. Brochier-Armanet, L. Loiseau, E. Talla, F. Barras, Iron–sulfur (Fe/S) protein biogenesis: phylogenomic and genetic studies of A-type carriers, PLoS Genet. 5 (2009) e1000497.
[125] D.T. Mapolelo, B. Zhang, S. Randeniya, A.N. Albetel, H. Li, J. Couturier, C.E. Outten, N. Rouhier, M.K. Johnson, Monothiol glutaredoxins and A-type proteins: partners in Fe–S cluster trafficking, Dalton Trans. 42 (2013) 3107–3115.
[126] J. Zeng, M. Geng, H. Jiang, Y. Liu, J. Liu, G. Qiu, The IscA from *Acidithiobacillus ferrooxidans* is an iron–sulfur protein which assemble the [Fe4S4] cluster with intracellular iron and sulfur, Arch. Biochem. Biophys. 463 (2007) 237–244.
[127] I. Cozar-Castellano, M. del Valle Machargo, E. Trujillo, M.F. Arteaga, T. Gonzalez, P. Martin-Vasallo, J. Avila, hIscA: a protein implicated in the biogenesis of iron–sulfur clusters, Biochim. Biophys. Acta 1700 (2004) 179–188.
[128] K. Cai, R.O. Frederick, J.H. Kim, N.M. Reinen, M. Tonelli, J.L. Markley, Human mitochondrial chaperone (mtHSP70) and cysteine desulfurase (NFS1) bind preferentially to the disordered conformation whereas co-chaperone (HSC20) binds to the structured conformation of the iron–sulfur cluster scaffold protein (ISCU), J. Biol. Chem. 288 (2013) 28755–28770.
[129] A.C. Adam, C. BornhÖvd, H. Prokisch, W. Neupert, K. Hell, The Nfs1 interacting protein Isd11 has an essential role in Fe/S cluster biogenesis in mitochondria, EMBO J. 25 (2006) 174–183.
[130] Y. Shi, M.C. Ghosh, W.H. Tong, T.A. Rouault, Human ISD11 is essential for both iron–sulfur cluster assembly and maintenance of normal cellular iron homeostasis, Hum. Mol. Genet. 18 (2009) 3014–3025.
[131] N. Wiedemann, E. Urzica, B. Guiard, H. Muller, C. Lohaus, H.E. Meyer, M.T. Ryan, C. Meisinger, U. Muhlenhoff, R. Lill, N. Pfanner, Essential role of Isd11 in mitochondrial iron–sulfur cluster synthesis on Isu scaffold proteins, EMBO J. 25 (2006) 184–195.
[132] Y.X. Shan, E. Napoli, G. Cortopassi, Mitochondrial frataxin interacts with ISD11 of the NFS1/ISCU complex and multiple mitochondrial chaperones, Hum. Mol. Genet. 16 (2007) 929–941.
[133] J. Bridwell-Rabb, N.G. Fox, C.L. Tsai, A.M. Winn, D.P. Barondeau, Human frataxin activates Fe–S cluster biosynthesis by facilitating sulfur transfer chemistry, Biochemistry 53 (2014) 4904–4913.
[134] J. Bridwell-Rabb, C. Iannuzzi, A. Pastore, D.P. Barondeau, Effector role reversal during evolution: the case of frataxin in Fe–S cluster biosynthesis, Biochemistry 8 (2012).
[135] N. Maio, A. Singh, H. Uhrigshardt, N. Saxena, W.H. Tong, T.A. Rouault, Cochaperone binding to LYR motifs confers specificity of iron sulfur cluster delivery, Cell Metab. 19 (2014) 445–457.
[136] J.R. Cupp-Vickery, H. Urbina, L.E. Vickery, Crystal structure of IscS, a cysteine desulfurase from *Escherichia coli*, J. Mol. Biol. 330 (2003) 1049–1059.
[137] P.W. Bilder, H. Ding, M.E. Newcomer, Crystal structure of the ancient, Fe–S scaffold IscA reveals a novel protein fold, Biochemistry 43 (2004) 133–139.
[138] J.R. Cupp-Vickery, J.J. Silberg, D.T. Ta, L.E. Vickery, Crystal structure of IscA, an iron–sulfur cluster assembly protein from *Escherichia coli*, J. Mol. Biol. 338 (2004) 127–137.
[139] D. Xu, G. Liu, R. Xiao, T. Acton, S. Goldsmith-Fischman, B. Honig, G.T. Montelione, T. Szyperski, NMR structure of the hypothetical protein AQ-1857 encoded by the Y157 gene from *Aquifex aeolicus* reveals a novel protein fold, Proteins 54 (2004) 794–796.
[140] Y. Shimomura, Y. Takahashi, Y. Kakuta, K. Fukuyama, Crystal structure of *Escherichia coli* YfhJ protein, a member of the ISC machinery involved in assembly of iron–sulfur clusters, Proteins 60 (2005) 566–569.
[141] S.J. Cho, M.G. Lee, J.K. Yang, J.Y. Lee, H.K. Song, S.W. Suh, Crystal structure of *Escherichia coli* CyaY protein reveals a previously unidentified fold for the evolutionarily conserved frataxin family, Proc. Natl. Acad. Sci. U. S. A. 97 (2000) 8932–8937.
[142] M. Nair, S. Adinolfi, C. Pastore, G. Kelly, P. Temussi, A. Pastore, Solution structure of the bacterial frataxin ortholog, CyaY: mapping the iron binding sites, Structure 12 (2004) 2037–2048.
[143] Y.N. He, S.L. Alam, S.V. Proteasa, Y. Zhang, E. Lesuisse, A. Dancis, T.L. Stemmler, Yeast frataxin solution structure, iron binding, and ferrochelatase interaction, Biochemistry 43 (2004) 16254–16262.
[144] T. Karlberg, U. Schagerlof, O. Gakh, S. Park, U. Ryde, M. Lindahl, K. Leath, E. Garman, G. Isaya, S. Al-Karadaghi, The structures of frataxin oligomers reveal the mechanism for the delivery and detoxification of iron, Structure 14 (2006) 1535–1546.
[145] C.A. Soderberg, A.V. Shkumatov, S. Rajan, O. Gakh, D.I. Svergun, G. Isaya, S. Al-Karadaghi, Oligomerization propensity and flexibility of yeast frataxin studied by X-ray crystallography and small-angle X-ray scattering, J. Mol. Biol. 414 (2011) 783–797.

[146] C.A. Soderberg, S. Rajan, A.V. Shkumatov, O. Gakh, S. Schaefer, E.C. Ahlgren, D.I. Svergun, G. Isaya, S. Al-Karadaghi, The molecular basis of iron-induced oligomerization of frataxin and the role of the ferroxidation reaction in oligomerization, J. Biol. Chem. 288 (2013) 8156–8167.
[147] S. Dhe-Paganon, R. Shigeta, Y.I. Chi, M. Ristow, S.E. Shoelson, Crystal structure of human frataxin, J. Biol. Chem. 275 (2000) 30753–30756.
[148] G. Musco, G. Stier, B. Kolmerer, S. Adinolfi, S. Martin, T. Frenkiel, T. Gibson, A. Pastore, Towards a structural understanding of Friedreich's ataxia: the solution structure of frataxin, Structure 8 (2000) 695–707.
[149] J.R. Cupp-Vickery, L.E. Vickery, Crystal structure of Hsc20, a J-type Co-chaperone from *Escherichia coli*, J. Mol. Biol. 304 (2000) 835–845.
[150] E. Bitto, C.A. Bingman, L. Bittova, D.A. Kondrashov, R.M. Bannen, B.G. Fox, J.L. Markley, G.N. Phillips Jr., Structure of human J-type co-chaperone HscB reveals a tetracysteine metal-binding domain, J. Biol. Chem. 283 (2008) 30184–30192.
[151] Y. Kakuta, T. Horio, Y. Takahashi, K. Fukuyama, Crystal structure of *Escherichia coli* Fdx, an adrenodoxin-type ferredoxin involved in the assembly of iron–sulfur clusters, Biochemistry 40 (2001) 11007–11012.
[152] S. Rajagopalan, S.J. Teter, P.H. Zwart, R.G. Brennan, K.J. Phillips, P.J. Kiley, Studies of IscR reveal a unique mechanism for metal-dependent regulation of DNA binding specificity, Nat. Struct. Mol. Biol. 20 (2013) 740–747.
[153] J.A. Santos, N. Alonso-Garcia, S. Macedo-Ribeiro, P.J. Pereira, The unique regulation of iron–sulfur cluster biogenesis in a Gram-positive bacterium, Proc. Natl. Acad. Sci. U. S. A. 111 (2014) E2251–E2260.
[154] H. Theyssen, H.P. Schuster, L. Packschies, B. Bukau, J. Reinstein, The second step of ATP binding to DnaK induces peptide release, J. Mol. Biol. 263 (1996) 657–670.
[155] C.J. Harrison, A.A. Bohm, H.C. Nelson, Crystal structure of the DNA binding domain of the heat shock transcription factor, Science 263 (1994) 224–227.
[156] S.V. Slepenkov, S.N. Witt, Kinetics of the reactions of the *Escherichia coli* molecular chaperone DnaK with ATP: evidence that a three-step reaction precedes ATP hydrolysis, Biochemistry 37 (1998) 1015–1024.
[157] D. Schmid, A. Baici, H. Gehring, P. Christen, Kinetics of molecular chaperone action, Science 263 (1994) 971–973.
[158] D. Franke, D.I. Svergun, DAMMIF, a program for rapid ab-initio shape determination in small-angle scattering, J. Appl. Crystallogr. 42 (2009) 342–346.